Slovak Geol. Mag., 8, 1(2002), 65 – 87

HP rocks associated with mylonitoclasites: a result of polystage overprint of the Austro-Alpine basement (Kreuzeck Massif, Eastern Alps)

MARIÁN PUTIŠ [1], SERGUEI P. KORIKOVSKY[2], WOLFGANG UNZOG[3] & NIELS OE. OLESEN

[1]J.A. Comenius University of Bratislava, Faculty of Natural Sciences, Dept. of Mineralogy and Petrology, Mlynská dolina, SK-84215 Bratislava, Slovak Republic, *Corresponding author. *Fax*: +421-2-60296293, *E-mail address*: putis@fns.uniba.sk
[2]Russian Academy of Sciences, Institute of Geology of Ore Deposits, Petrography, Mineralogy and Geochemistry, Staromonetny per. 35, 109017 Moscow, Russian Federation.
[3]K.F. University of Graz, Institute of Geology and Paleontology, Heinrichstr. 26, A-8010 Graz, Austria.
[4]University of Aarhus, Faculty of Science, Dept. of Earth Sciences, Nordre Ringgade 1, DK-8000 Aarhus, Denmark.

Abstract. The studied region of the Kreuzeck Massif southeast of the Tauern Window in the Austrian Eastern Alps reveals contrasting early-Cretaceous overprint of the Austro-Alpine (AA) basement complexes from (sub-) greenschist- to HP amphibolite/eclogite facies. An unusuall association of HP rocks with mylonitoclasites have been found along early-Tertiary lateral strike slip-fault shear zone within the Kreuzeck Massif.

Petrofabrics of strongly overprinted (reactivated) rocks from the pre-Alpine basement were used for identification of micromechanisms of brittle-ductile deformation and reconstruction of P-T conditions related to subductional burial and exhumation of HP and MP fragments recently located within the Tertiary dextral strike slip shear zone. The HP amphibolites to eclogites (?) and the host kyanite-garnet paragneisses and granitic orthogneisses form tectonic lenses of the AA Polinik structural complex along this shear zone. The rocks often show ductile deformation and dynamic recrystallization of plagioclase and quartz, while amphibole and pyroxene were subjected to reaction recrystallization. Ductile (plagioclase-quartz) fabrics in barroisite- and clinopyroxene (high-Na augite)- bearing HP amphibolites to eclogites (?) postdate metamorphic HP/MT fabrics. Calculated temperature of (Cretaceous) collisional metamorphism is ca. 530 °C at minimum pressure of 11 kbar. No relics of pre-Alpine fabrics have been preserved in the Polinic structural complex.

Variscan metamorphic assemblage of the AA Strieden structural complex (staurolite, garnet, andalusite, sillimanite, plagioclase, formed at T_{max} around 600 °C and 4-5 kbar of P) is discernible outside the strike slip shear zone. Approaching this zone, the degree of Alpine overprint is increasing according to newly-formed assemblage of chloritoid, margarite, albite, garnet-outer zone, which represents (Cretaceous) T_{max} of ca. 500 °C and 6-7 kbar of P. Structurally rebuilt northern part of the AA Strieden complex, adjoining the (early-Tertiary) shear zone, shows simultaneous micromechanisms of mylonitic (ductile) flow in quartz and mylonitic-cataclastic flow in feldspars of ortho- and paragneisses. Similarly, marbles show mechanical differences in alternating mylonitic calcite and mylonitic-cataclastic dolomite layers. This seems to be typical of frictional-viscous flow producing mylonitoclasites. The measured (plagioclase, quartz, calcite, dolomite) mineral textural patterns are related to dextral strike slip or top-to-WNW shifting of steeply south-dipping AA basement fragment.

Reactivated HP/MP AA basement fragments, finally exhumed in the early-Tertiary dextral strike slip fault shear zone, might be the fragments coming from Cretaceous continental subduction zone. The exhumed overprinted rocks were intruded by volcanic dykes ca. 32 Ma old, the latter being cut by (Miocene) ultracataclasites.

Keywords: HP rocks; mylonitoclasite; P-T path; polystage overprint; Eastern Alps

1. Introduction

The reviews of exhumation mechanisms of high-pressure (HP) rocks have been provided by Droop et al. (1990), Ring (1992), Platt (1993), Gebauer et al. (1993), Dal Piaz et al. (1993), Froitzheim et al. (1996), Spalla et al. (1996), Kurz and Neubauer (1998), Dal Piaz (1999), Putiš et al. (2000, 2002) mainly on the examples from the Alps using mineral and microstructural changes.

A few principal micromechanisms enhance a crustal volume to be exhumed in form of a tectonic fragment along a shear zone. The deeper horizons are characteristic of higher temperatures, lower strain rates and thus lower lithosphere strengths (rigidity) in deformation. There, a micromechanism of grain-size insensitive creep (e.g. Barber, 1990) is characteristic with lower values of shear strength or flow stress. Mylonitic rocks in the shear zones, therefore coincide with a crustal strength minimum and enhance development of a detachment fault. The shallower horizons can accommodate a transitional frictional-viscous flow (Handy et al., 1999) producing clastomylonites or mylonitoclasites depending on a volume share of mylonitic vs. cataclatic matrix. Mylonitoclasites indicate lowering temperatures at increasing deformation rates. At the same time, the lithosphere strength is increasing towards dominated frictional flow in the upper crust.

Solution of exhumation mechanisms in the Kreuzeck Massif of central Eastern Alps was initiated by findings of eclogitic metabasics (Hoke, 1990) within the Austro-Alpine (AA) basement complexes in close association with mylonites, mylonitoclasites to ultracataclasites. Such unusual rock association indicates a polystage evolution of strongly deformed (overprinted) basement rocks. The local situation can be explained by predominated Cretaceous internal structure of the AA basement that is overprinted by superposed Tertiary tectonic structures, especially steeply

south dipping dextral (top-to-WNW) strike slip fault zones (Ratschbacher et al., 1991; Frisch et al., 1999; Mancktelow et al., 1999) truncating the studied Kreuzeck Massif area (Fig. 1).

The Austro-Alpine (AA) basement structural complexes represent an orogenic wedge (Platt, 1993) of continental crust that formed during the Early Cretaceous collision (Neubauer, 1994; Dallmeyer et al., 1998) fol-

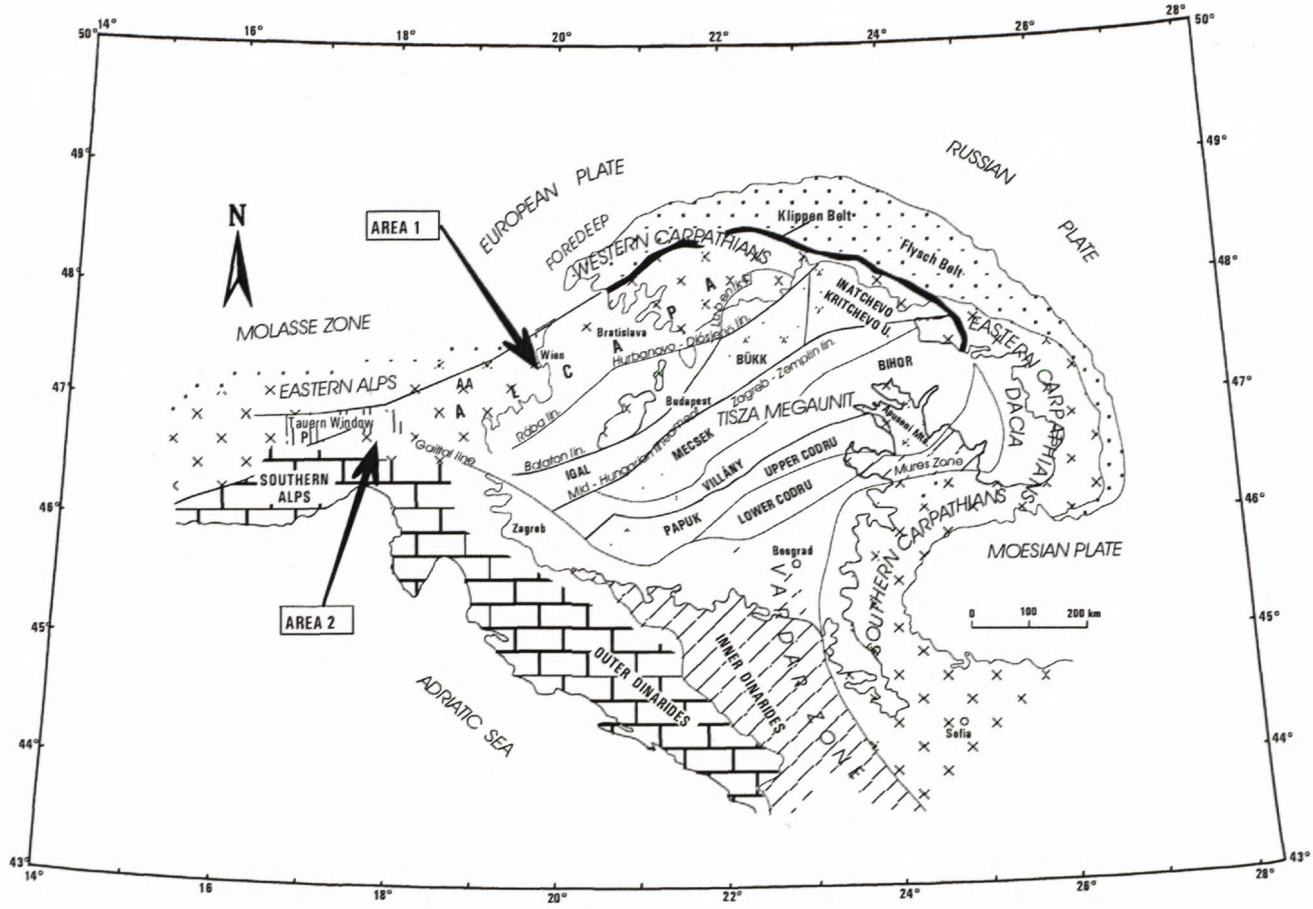

*Fig. 1. Tectonic sketch map of the East **Al**pine-**Ca**rpathian-**Pa**nnonia (ALCAPA) orogen with position of the Austro-Alpine (AA) unit (after Plašienka et al., 1997). Area 1: documents subhorizontally stacked AA structural complexes due to Early Cretaceous collision (include the Middle AA structural complex with Cretaceous eclogites,). Area 2: The Kreuzeck Massif AA structural complexes piled up S of the Tauern Window undergone to Late Cretaceous-Tertiary transpression and normal faulting.*

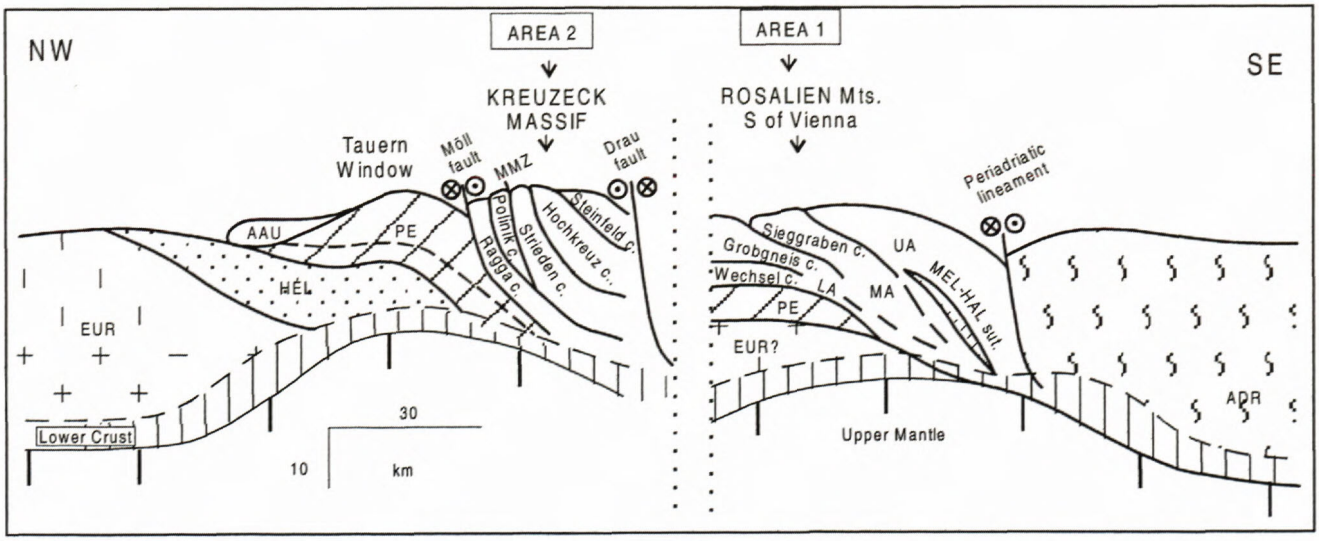

Fig. 2. Schematic tectonic cross-section of the Austro-Alpine unit (modified fig. 2 from Putiš et al., 2002). EUR=European plate, HEL=Helvetic zone, PE=Pennine zone, AAU=Austro-Alpine unit, LA=Lower AA, MA= Middle AA, UA=Upper AA, MEL-HAL sut.=Meliata-Hallstatt ocean suture zone, ADR = Adria (or Apulia) microplate.

lowing the closure of the Meliata-Halstatt ocean in the Late Jurassic. This event caused an extreme shortening of the AA unit and juxtaposed different structural complexes metamorphosed in eclogite to (sub)greenschist facies cropping out in the Kreuzeck Massif at the distance of a few kilometres (Fig. 2, 3).

The AA complexes (Tollmann, 1977) occupied a lower plate position during the Late Jurassic-Early Cretaceous collision, but the upper plate position during the Late Cretaceous-Tertiary collision. In the former case, they participated in shortened early Tethyan Meliata-Hallstatt passive continental margin. In the latter case, following the closure of the Pennine ocean, the AA unit became frontal part of the Apulia (Adria) indenter, which collided with the European passive continental margin (Kozur, 1991; Neubauer, 1994; Stampfli, 1996; Froitzheim et al., 1996; von Blanckenburg and Davies, 1996; Dallmeyer et al., 1996; Stampfli and Mosar, 1999; Dal Piaz, 1999; Putiš et al., 2000, 2002). The studied regional tectonic structure developed by subhorizontal nappe thrusting that transformed to subvertical dextral (transpression?) strike slip and steepening the nappe slices. Some of the basement fragments, usually rich in metabasics, metaultrabasics, marbles along with metapelites, less granite gneisses, underwent even continental subduction in HP amphibolite- or eclogite facies P-T conditions (reviewed by Putiš et al., 2002).

The purpose of this paper is to document the function of a brittle-ductile shear zone that enhanced final exhumation of early-Alpine HP to MP rocks during earlier stages of Tertiary strike slip-fault tectonics following the collision between the AA and Pennine units in the Eastern Alps. We revealed principal characteristics and evolution steps of strain-accommodating minerals, including their textural patterns from the Kreuzeck Massif strike slip shear zone, and compared them to those from the normal-fault shear zone (dated 20-15 Ma, Cliff et al., 1985; Selverstone, 1988) at the eastern edge of the Pennine Tauern Window. While the reconstructed petrological P-T path is related to early-Alpine exhumation stage of HP/MP AA basement fragments, mechanical behaviour and kinematics of polymineralic mylonites seem to be related to brittle-ductile deformation along the early-Tertiary steeply south dipping shear zone. The paper shows varying early-Alpine reactivation grades of pre-Alpine basement fragments (AA structural complexes) crosscut by early-Tertiary dextral exhumation shear zone. Polystage exhumation of reactivated basement fragments has been studied using microstructural and petrological methodological approaches.

2. Geological structure of the Kreuzeck Massif

2.1. Geological structure of the Kreuzeck Massif from the viewpoint of former investigations

Hoke (1990) published examples of the deformation styles of mesostructures and their relationship to metamorphic and mylonitic events from the northwestern part of the Kreuzeck Massif. Her´s results point to Cretaceous remetamorphism of the AA basement in the time interval around 100-90 Ma (a few K-Ar and Rb-Sr data). Oxburg et al. (1966) found a lot of 83-76 Ma (K-Ar ages on muscovite and biotite), or even younger 66 Ma (one age on muscovite and one on biotite) mineral ages at the boundary with the Tauern Window Pennine unit. An age of 61 Ma was found at the southern boundary with the main mylonite zone directly in the Kreuzeck Massif (MMZ, Hoke, 1990).

There are two different structural-metamorphic domains from the view-point of Alpine overprint (reactivation) in the Kreuzeck Massif built of AA structural complexes: the domain north of the MMZ with the Late Cretaceous K-Ar muscovite and biotite ages; and the domain south of the MMZ with the well preserved pre-Alpine (late-Variscan) K-Ar ages. Hoke (1990) included the northern domain into the Polinik unit and the southern one into the Strieden unit on the basis of the work in the area between the Möll valley and Strieden and Polinik Mt. peaks. She proposed amphibolite to eclogite facies Alpine reactivation in the Polinik, but only the lower greenschist-facies in the Strieden unit (Hoke, 1990, fig. 47).

The apatite FT ages (Staufenberg, 1987) of the Polinik AA complex are ranging from 6 to 23.4 Ma, likewise in the neighbouring Pennine Tauern Window. However the data from the southern „Altkristallin" of the Kreuzeck Massive yield higher cooling ages up to 31.4 Ma, rarely approaching even 40 Ma, indicating the existence of separated blocks. This fact stresses the importance of the Möll, Drau and MMZ fault system (Fig. 2-4) during the Tertiary tectogenesis.

The lowest-T evolution period is also documented by zircon FT ages from the different structural complexes of the tectonostratigraphical nappe pile proposed by Putiš et al. (1997a) and described in the paragraph below. The zircon FT ages of the AA unit south of the Tauern Window yield a wide interval of 84-35 Ma (Frisch et al., 1999) reflecting different Mesozoic (Eoalpine, Cretaceous) and Tertiary tectonic blocks.

The strongly reactivated higher-grade metamorphic Variscan basement structural complexes („Altkristallin") with the occurrences of Alpine amphibolites to eclogites were mapped also westwards of the Kreuzeck group – in the Schober group and mentioned in published short reports (Putiš et al., 1996, 1997a; Linner; 1997, Spaeth, 1997) on manuscripts to geological maps deposited in the Austrian Geological Survey in Vienna.

The new Metamorphic Map of the Eastern Alps (Hoinkes et al., 1999) does not yet contain all the newest, findings of the eclogitic rocks and the picture of the metamorphism in the AA complexes can be precised in the area of question.

2.2. Geological structure of the Kreuzeck Massif based on the new investigations

The new compiled map of the Kreuzeck Massif (Fig. 3, after Putiš, 1998) and the published report (Putiš et al., 1997a) to this map yield a view on the whole Alpine tectonic structure of the Kreuzeck Massif S of the Tauern

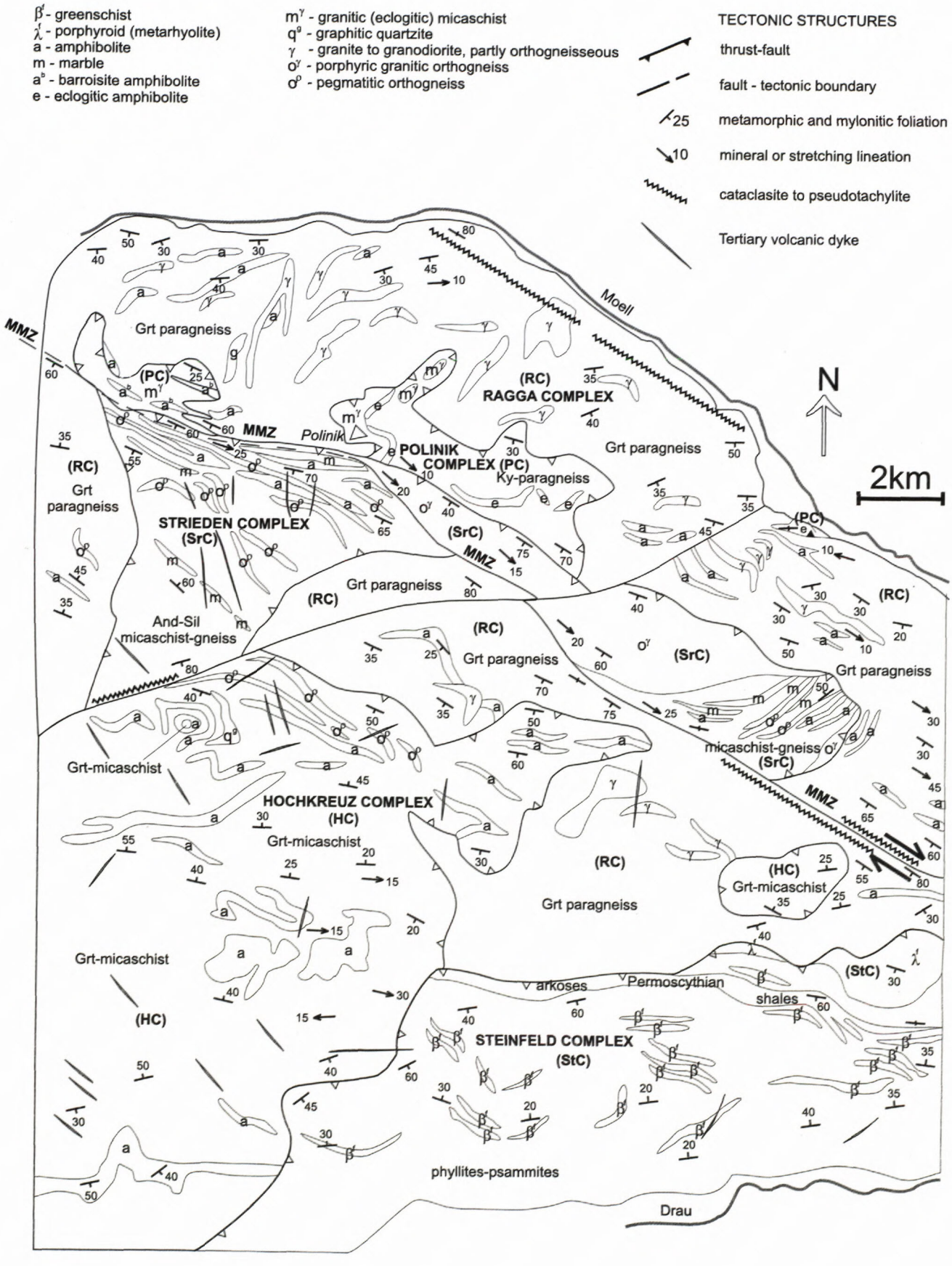

Fig. 3 Compiled geological-structural map of the central part of the Kreuzeck Massif (after Putiš et al., 1995-1997 and Putiš, 1997).

Window. The mapping work (Putiš et al., 1995, 1996, 1997b) revealed at least 5 stacked AA structural complexes (basement nappes) built of characteristic lithological members. They are (from north and tectonic bottom): the Ragga structural complex (gneisses, amphibolites, migmatites, partly orthogneisseous granitoids), the Polinik structural complex (Ky-St-Grt gneisses, eclogitic high-Na augite amphibolites and Bar-bearing amphibolites, granitic feldspar-gneisses to micaschits, leucocrate granitic gneisses), the Strieden structural complex (Sil-And paragneisses and St-Grt micaschist gneisses, associated with Grt amphibolites, Cal-Dol-Tr marbles, small pegmatitic and large porphyric granitic gneisses), the Hochkreuz structural complex (micaschists, graphitic quartzites, large amphibolitic, gabbro-amphibolitic to layered amphibolitic bodies) and the Steinfeld structural complex (metapelites, metagreywackes, greenschists, porphyroids, Cld schists) covered by slightly (anchi-)metamorphosed Permo-Scythian sediments (arkoses, shales, quartzites).

According to our field work, the HP amphibolite facies (Cretaceous ?) metamorphism of the Polinik structural complex is restricted in the studied area along the MMZ and around the Polinik Mt. peak. Because of this reason, the rest of the former Polinik unit (defined by Hoke, 1990) further to north was included into the newly-defined Ragga structural complex showing only greenschist facies Alpine overprint (Putiš et al., 1997a, b).

The HP Polinik- and MP Strieden complexes are „rooted" in dextral strike slip shear zone, which is considered to be their exhumation „suture„ (Putiš et al., 1998). It is located between the underlying gneiss-migmatite-granitic Ragga complex (present in the front of the AA nappe complex) and overlying Hochkreuz-Steinfeld complexes.

The types of mesostructures and their orientations are depicted in schematic structural-geological map (Fig. 3). Foliations and lineations outside the MMZ are mostly pre-Alpine metamorphic elements partly modified during the Alpine deformations. The MMZ, on the other hand, is characterized by subparallel mylonitic foliations, mineral and stretching lineations. In places, the older foliation is preserved in form of S-planes in S-C mylonites (Berthé et al., 1979) indicating top-to-WNW shear. Internal structure of this zone striking WNW-ESE is characterized by steeply dipping foliations and oblique to subhorizontal stretching lineations of strongly mylonitic rocks. The whole structure is cut by mostly NNW-SSE trending volcanic dykes dated 32-35 Ma (Deutsch, 1984). They are well fitting to dextral kinematics and the brittle-ductile stage of deformation.

The neighbouring Pennine Reisseck Massif is separated from the AA Kreuzeck Massif by a dextral strike slip fault zone (Ratschbacher et al., 1991), while an extensional normal fault boundary was found by Genser and Neubauer (1989) in the easternmost part of the Reisseck

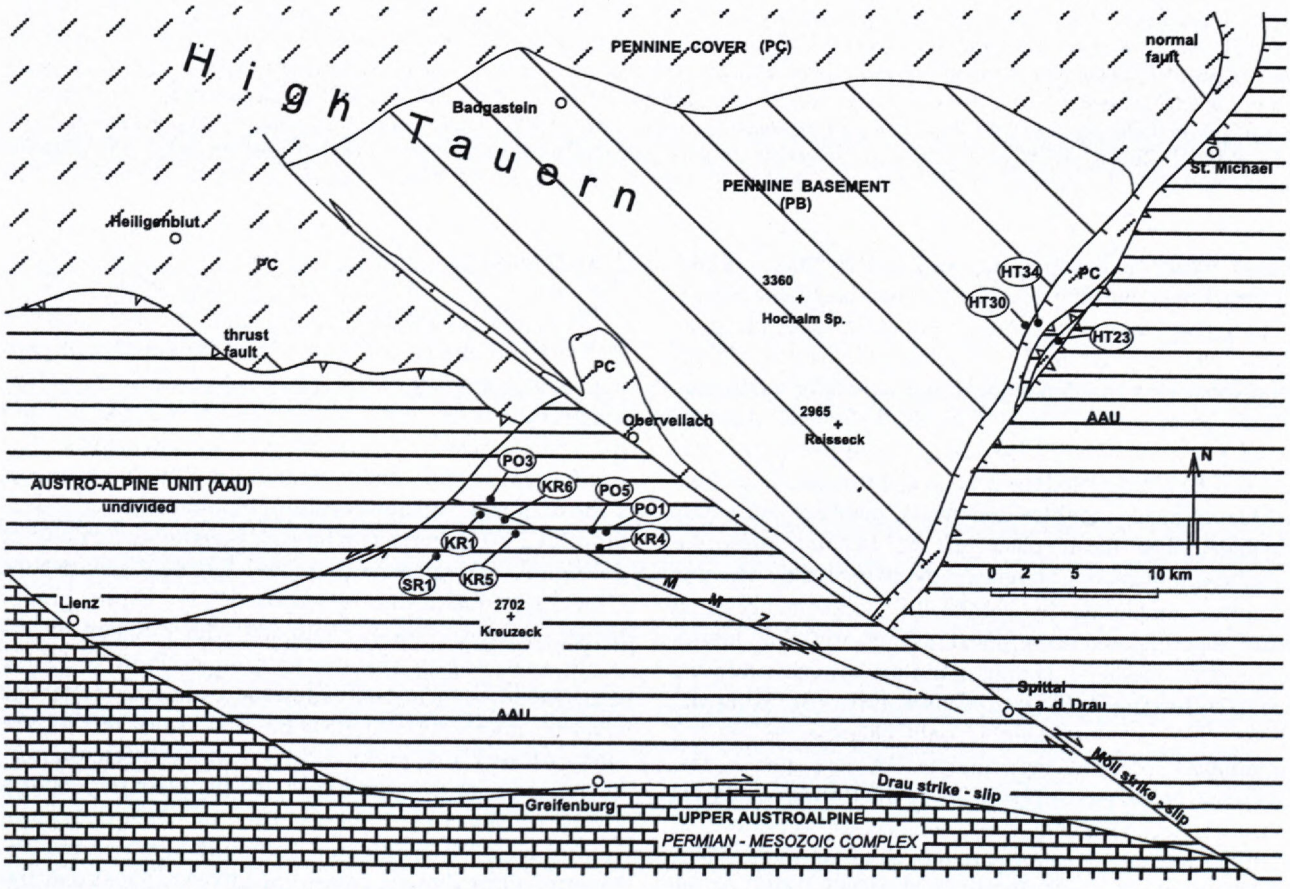

Fig. 4. Geological-tectonic sketch-map of the southeastern margin of the Tauern Window and Kreuzeck Massif in the Area 2, include the samples location. Austro-Alpine unit (AAU) is undivided. Pennine basement complex (PB). Pennine cover complex (PC).

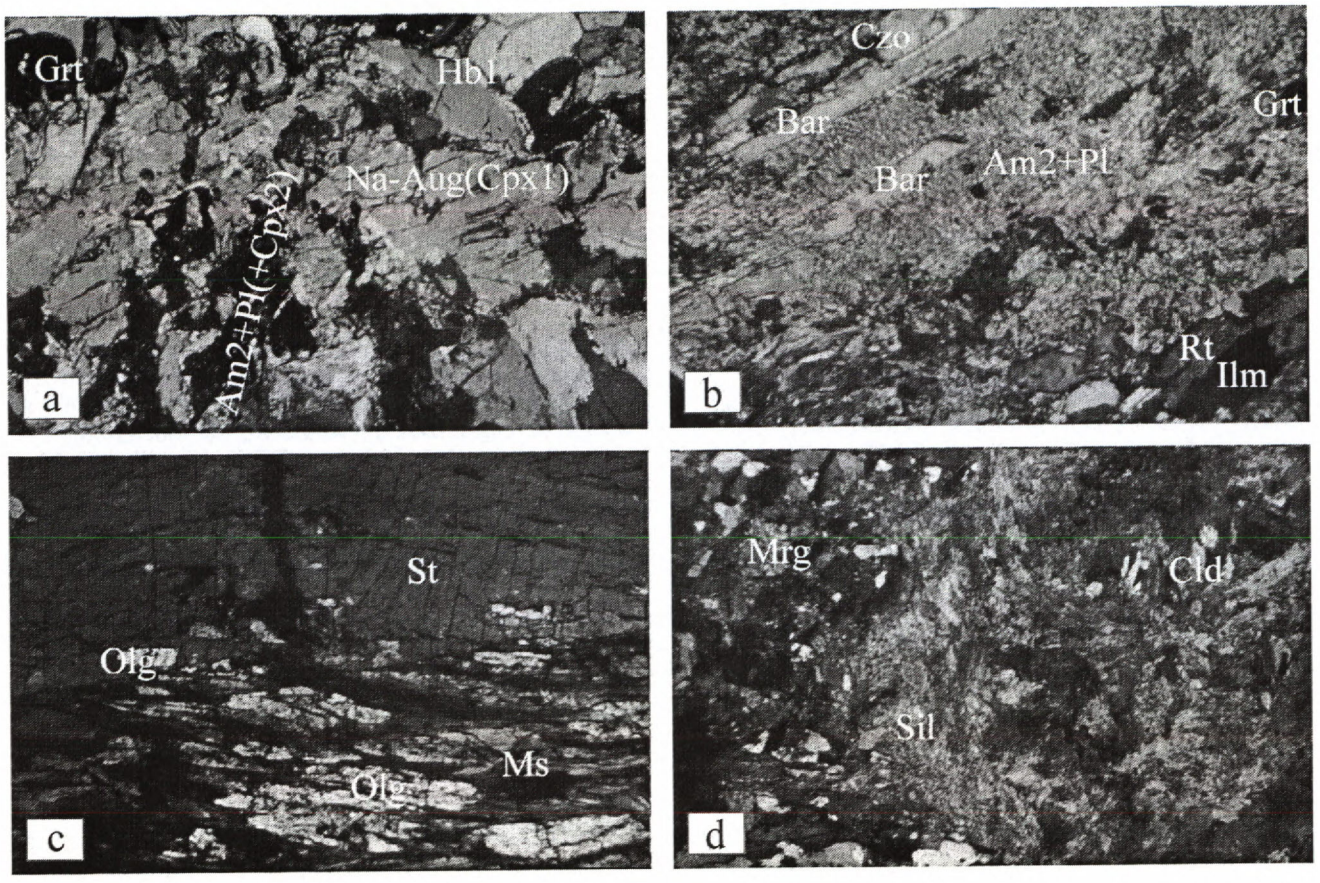

Fig. 5. Microstructures of metamorphic minerals of the Polinik (a, b) and Strieden (c, d) structural complexes. Sample-location according to Fig. 4. (a) High-Na Aug, Hb1 (D1 Alpine); post-peak Am2, Pl, and rare Cpx2 symplectitic aggregates (D2 Alpine), HP amphibolite. (b) Bar (HP) amphibole prismatic crystalls associated with Grt, Rut and Czo (D1 Alpine); symplectites of Am2 (Prg-, Ed-Prg-, or Ed-Act) and Olg associated with Ilm, Chl, Ep (D2 Alpine). (c) Late syntectonic St porphyroblast enclosing metamorphic schistosity with Olg, Ms, Bt and Qtz. (d) Snowball shaped Sil porphyroblasts associated with Bt (Variscan) and the superimposed (Alpine) recrystallization products: Cld, Ms and Mrg. (e) BSE image of symplectite from eclogitic amphibolite of the Polinik complex (s. PO5). (f) BSE image of symplectite from Bar HP amphibolite of the Polinik complex (s. PO3). Magnification: 18x (a, c), 25x (b), 30x (d).

Massif, where the Pennine unit merges below the overthrust Austro-Alpine one (Fig. 4). The Pennine basement is built of porphyric „Zentralgneis"-type granitoids and less migmatitic gneisses. The overlying Pennine Mesozoic rocks are subdivided into two lithological and structural complexes (Bezák et al., 1995): the 1st one is the lower, volcano-sedimentary complex (Bt-Ep-Ab, Qtz-Ab-Phe-Chl, Ab-Ep-Chl-Hbl-Bt schists), and the 2nd one is the upper, calcschist-marble complex (marbles and marly marbles, calcareous phyllites). The thrust plane of the Pennine Mesozoic volcano-sedimentary complex overlying the Pennine basement complex is dipping 20-40° to the southeast. It bears superimposed extensional asymmetric S-C fabrics indicating a top-to-SE sliding along the distinct stretching lineation striking NW-SE to WNW-ESE (Bezák et al., 1995). Such tectonic style is only characteristic in the easternmost edge of the window, because just a few kilometres to the west, everywhere in the Pennine besement of the Reisseck-Hochalm Massif the NW-SE to NNW-SSE striking stretching lineations are related to top-to-the NW(-NNW) nappe transport (Bezák et al., 1993, 1994) of the inferred older age (60 Ma?), compairing e.g. the results of Kurz et al. (1998) further to west.

3. Methodology

The newly-outlined geological-structural scheme (Fig. 3) was drawn on the basis of detailed field geological mapping (the Austrian Geological Survey mapping project 1995-1997, attended by M. Putiš et al.) and the complementary structural-petrological studies. The applied research methods embody the study of microstructures and mineral crystallographic preferred orientation (CPO) patterns (textures) of quartz and calcite or dolomite aggregates using the U-stage microscope (Univ. of Bratislava), reflection X-ray texture goniometer (Univ. of Graz), combined with electron microprobe analysing of rock-forming minerals of mylonitic rocks and some thermobarometric estimates. CamScan electron microscope in BSE mode was utilized for the study of very fine-grained deformed aggregates (Univ. of Aarhus), or for the study of symplectitic textures (Univ. of Moscow). EDS was used for identification or confirmation of calcitic and dolomitic layers in marble. Mineral abbreviations (see Appendix A) in text and figures are used after Kretz (1983) and end-members of Ca-amphiboles after Leake et al. (1997).

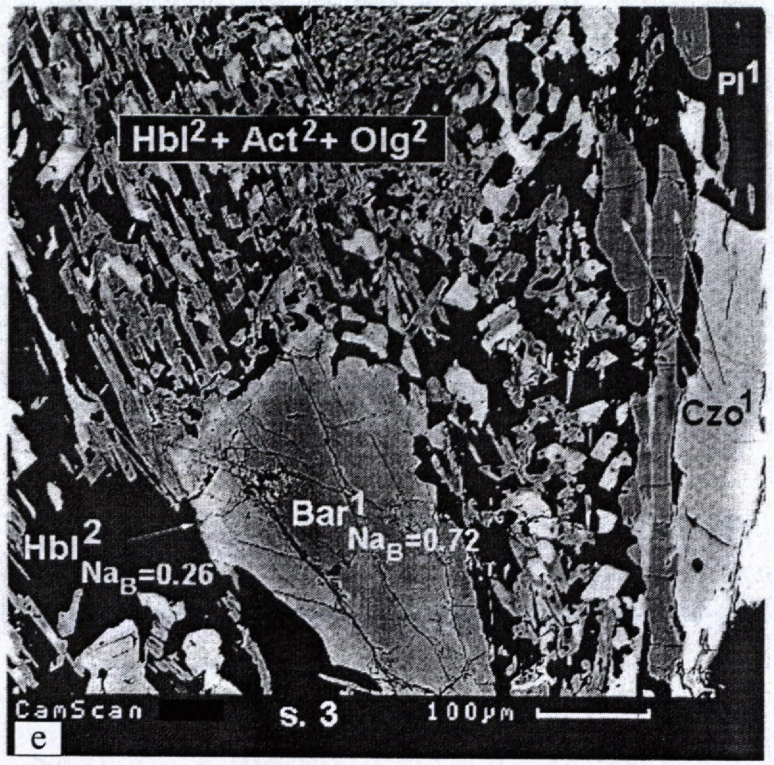

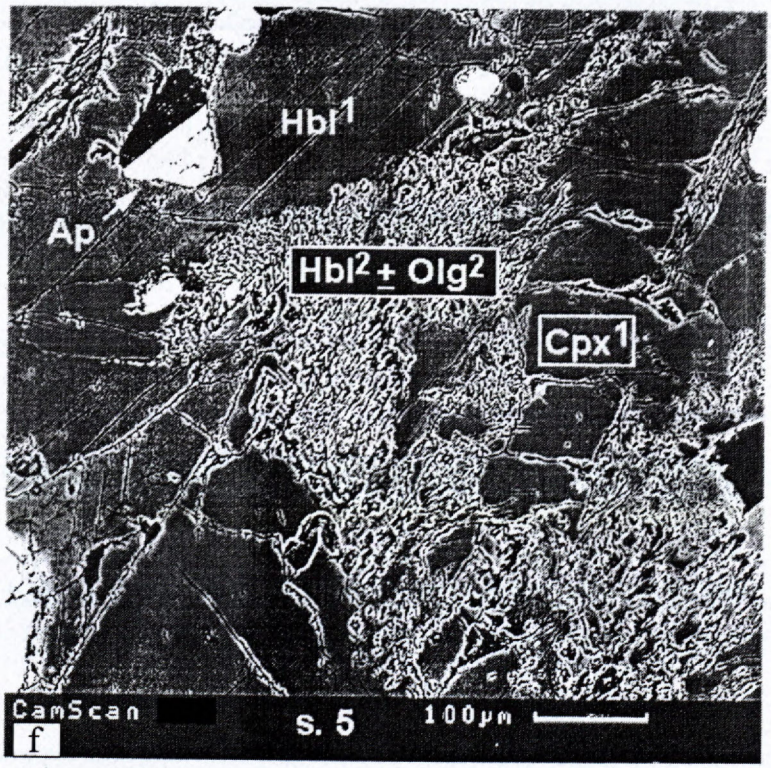

of the complex along the transpression exhumation shear zone („suture").

Eclogitic amphibolites contain Alm (50-55%)-Prp (18-24%)-Grs(20-29%) garnet (Tab. 1) associated with high-Na Aug (=Cpx1, with the maximum 22 % of Jd, Tab. 2, Fig. 5a), Mg-Hbl1 (Tab. 3, Fig. 5a), and rare Bt1. The real eclogites (with the true Omp) have not yet been discovered. Black symplectitic rims around Cpx1 are composed of Mg-Hbl2+Olg, occasionally Cpx2(with ca. 5 to 3 % of Jd, Tab. 2, Fig. 5a). The symplectite replacement usually occupies only part of the Cpx1 boundary with Grt. Al-rich Prg to Ts amphiboles (Hbl2) (Tab. 3) form often the reaction rims around Grt; but Hbl2 from symplectites (Fig. 5e) around Cpx1 are represented by Al-poor Act-Hbl amphiboles. Garnet grains in eclogitic amphibolites have only a prograde zoning (Tab. 1) from core to rim, with increasing Prp content from 19 to 24 %, and decreasing Grs content from 28-29 to 19-21 %.

Grt-Hbl thermometry (Perchuk, 1989) using the Grt grains with Hbl(1) inclusions (Fig. 6 - s. PO5) revealed the prograde rise of T from 497 °C (cores of Grt) up to 533 °C (the outer zones). The maximum temperature of the burial stage has been obtained for contacts of Grt with adjoining Cpx1 and Hbl1: Grt (rim, with the maximum Prp content)+Na-Aug – 533 °C (Ai, 1994), and Grt (rim)+Hbl1 – 530 °C (Perchuk, 1989) (Fig. 6 - s. PO1). If the maximum Jd content in Cpx1 was 22 %, the minimum pressure at T ~ 530 °C deduced from the Jd isopleths in Cpx (Holland, 1980) was 11 kbar. Then the responding geothermal gradient during the D1 burial stage of the Cretaceous metamorphism of the Polinik complex was ca. 13 °C/km (Fig. 7). Decreasing T at the decreasing P is inferred for the D2 stage of the uplift, when the reactional Ts to Prg and Act-Hbl amphiboles have formed.

Some of metabasites contain Alm (48-50%)-Prp (25-28%)-Grs (20-23%) garnet (Tab. 4) associated with the Na-Ca amphibole (Am1) (Tab. 5, Fig. 5b), Czo, andesine-labradorite (Pl1) and single grains of Na-poor Kfs. Na-Ca amphibole is the Na-Ca barroisite (Leake et al., 1997) with NaB 0.60-0.73 per f.u., X Fe 0.31-0.34. Barroisite is replaced either by edenitic rims (NaB 0.09-0.33), or by the subparallel-oriented three-mineral symplectites (Fig. 5f) of edenite to pargasite (X Fe 0.37-0.48), actinolite (X Fe 0.23-0.29) (Tab. 5), and oligoclase (17-30% An). Ed to Prg and Act in these symplectites have often the sharp contacts, form the sepa-

4. Petrography and P-T estimates of the Polinik and Strieden structural complexes

4.1. Polinik structural complex

The Polinik complex shows the strongest Alpine overprint of former structures among AA basement complexes. This is compatible with position of tectonic lenses

Tab. 1. Microprobe analyses of zonal Grt containing inclusions of Hb. Grt-Cpx-Czo-Hb±Bt eclogitic amphibolite. Polinik structural complex. PO1 and PO5 samples location according to Fig. 4.

Sample	s. PO1 (Grt)					s. PO5 (Grt)						
						1-st grain				2nd grain		
Point	core				rim	core			rim	core		rim
SiO_2	38.48	38.44	38.32	38.06	38.23	37.80	38.06	38.20	38.04	38.15	38.13	38.39
TiO_2	0.06	0.09	-	-	-	0.14	0.07	0.06	-	0.14	0.08	0.05
Al_2O_3	21.66	21.95	21.69	21.70	22.15	21.89	21.97	21.53	21.86	21.48	21.99	21.81
FeO	23.77	23.46	25.59	25.98	25.27	24.30	24.73	24.51	26.70	25.12	25.25	26.31
MnO	0.33	0.46	0.41	0.49	0.37	0.56	0.42	0.46	0.55	0.72	0.61	0.40
MgO	5.18	5.02	5.52	6.23	6.30	4.95	4.78	4.91	5.63	4.80	5.23	6.17
CaO	10.16	10.50	8.20	7.52	7.66	10.21	9.92	10.25	7.21	9.33	8.65	6.77
Total	99.64	99.92	99.73	99.98	99.98	99.85	99.95	99.92	99.99	99.74	99.94	99.90
Si	3.01	2.98	3.00	2.97	2.97	2.97	2.97	2.98	2.97	3.00	2.97	2.99
Ti	-	0.01	-	-	-	0.01	-	-	-	0.01	0.01	-
Al	1.99	2.01	2.00	1.99	2.03	2.02	2.02	1.98	2.01	1.99	2.02	2.00
Fe	1.55	1.52	1.66	1.69	1.64	1.59	1.61	1.60	1.74	1.64	1.65	1.71
Mn	0.02	0.03	0.03	0.03	0.02	0.04	0.03	0.03	0.04	0.05	0.04	0.03
Mg	0.60	0.58	0.64	0.72	0.73	0.58	0.56	0.57	0.66	0.56	0.61	0.71
Ca	0.85	0.87	0.69	0.63	0.64	0.85	0.83	0.86	0.60	0.78	0.72	0.56
X_{Fe}	0.72	0.72	0.72	0.70	0.69	0.73	0.74	0.74	0.73	0.74	0.73	0.70
Alm	51.3	50.6	55.2	55.1	54.2	51.9	53.3	52.3	57.4	54.2	54.5	56.7
Sps	0.7	1.0	0.9	1.0	0.8	1.2	0.9	1.0	1.2	1.6	1.3	0.9
Prp	19.9	19.3	21.2	23.5	24.0	18.9	18.4	18.7	21.6	18.4	20.2	23.7
Grs	28.1	29.0	22.7	20.4	21.0	28.0	27.4	28.0	19.8	25.8	24.0	18.7

rate prisms, and most probably their simulateneous crystallization reflect the miscibility gap between them (Spear, 1982). Garnets are without inclusions, and the inner part of grains have the weak prograde zoning (increasing Prp content to outward from 26 to 29 %, and decreasing Grs from 23 to 20 %), and the retrograde zoning in the rims (an inverse behaviour of Prp and Grs, Tab. 4, Fig. 6 – s. PO3). Garnet grains are also replaced by very fine-grained „black" Al-pargasite (Tab. 5)-oligoclase/andesine-epidote kelyphitic rims. The strongly linear textures of symplectitic aggregates in Bar amphibolites are parallel to overall macroscopic subhorizontal stretching lineation of the Strieden complex within the transpression shear zone.

Owing to widespread formation of the reactional Hbl2-Ep2-Pl2 symplectites (Fig. 5b) always separating the Grt and Bar, the use of Grt-Hbl thermometry is problematic. Unfortunately, it is also impossible to use the Hbl-Grt-Pl-Qtz geobarometer because it is applicable (Kohn and Spear, 1990) only for associations containing the ordinary Ca-amphiboles, but not the Na-Ca barroisite.

The host rocks of metabasites are metapelites or Bt-Grt, St-Ky or Ky-Grt gneisses and migmatitic gneisses. The light-coloured mica-poor fine- to medium-grained orthogneiss bodies and medium- to coarse-grained orthogneisses represent original granitoid bodies within the metapelites. Some of them are feldspar-poor and resemble eclogitic micaschists.

4.2. Strieden structural complex

The Strieden complex shows variable degree of Alpine overprint, depending on distance from the MMZ (dexral strike slip shear zone). Deformation gradient culminates in fragments included into this deformation zone with predominating mineral assemblage of Alpine overprint. Such ductilely deformed rocks show subparallel fabrics and a unified kinematics with the exhumed HP rocks of the Polinik structural complex within the same shear zone. The latter fact speaks for common final exhumation of the HP Polinik and MP Strieden basement fragments.

In the Strieden complex Grt in all types of studied metapelitic/metapsammitic rocks (associated with normal amphibolites) have a prograde zoning along the whole profile (increasing Prp content from 5 % in the core to 10% in the rim); sometimes the prograde zoning is complicated by very narrow retrograde rims with an inverse - decreasing Prp content to 7-8 %. Grossular content is very low in garnets from Al-rich St-Grt schists (8 % in cores, and 3 % in the prograde rims), and it is high in Grt±Cal±Hbl-mica gneisses (about 22 % along the whole profile). Staurolite (Fig. 5c) is the Zn-poor (a maximum ZnO content is 0.12 wt. %), and it has the weak zoning (X Fe 0.85 in the core, and 0.88 in the rim). However Hoke (1990) found the St grains with outer Zn-rich zone that might be recrystallized older grains. Plagioclase in all types of rocks is oligoclase (10-24% An). Large flakes of the prograde Na-rich muscovite1 (X Na 0.24-0.25), and Bt (X Fe 0.47-0.62), together with oligoclase and quartz are the major minerals of the matrix. Among common Bt and Ms1, large flakes of the prograde chlorite1 (X Fe 0.52-0.57) are sometimes retained in matrix.

Grt-Bt geothermometry of St-Grt gneisses yields the maximum temperature of metamorphism at 614 °C

Tab. 2. Microprobe analyses of Cpx1 (large grains) and Cpx2 (from Hb2-Cpx2-Olg symplectites). Grt-Cpx-Czo-Hb±Bt eclogitic amphibolite. Polinik structural complex. PO1 and PO5 samples location according to Fig. 4.

Sample	s. PO5											s. PO1				
Type	Cpx^1 large grains								Cpx^2 from $Hb^2 \pm Cpx^2 \pm Olg^2$ rims			Cpx^1 large grains				
Name	sodic Aug								Aug			sodic Aug				
SiO_2	54.52	54.38	54.12	54.70	54.24	54.63	54.43	54.76	53.20	53.08	54.05	54.65	54.20	54.16	54.45	54.06
TiO_2	0.05	-	0.06	0.10	0.16	0.09	0.03	0.17	0.08	-	-	0.09	0.15	0.07	0.09	0.12
Al_2O_3	5.14	5.18	4.10	4.97	5.26	4.86	4.99	4.61	1.27	3.04	1.22	3.97	3.68	3.98	3.14	2.63
FeO	5.55	5.50	5.71	5.77	5.76	5.63	6.18	5.43	6.34	5.55	6.09	5.63	6.24	6.04	5.91	5.89
MnO	-	0.04	0.04	-	0.03	0.12	-	-	0.04	0.09	0.08	0.05	0.01	-	0.07	-
MgO	12.09	12.05	12.54	12.04	12.23	12.24	12.06	12.38	13.87	14.02	14.29	12.92	12.88	12.82	13.21	13.74
CaO	19.43	19.49	20.39	19.31	19.10	19.09	18.92	19.56	24.79	23.58	23.46	20.30	20.78	20.53	21.16	21.97
Na_2O	3.18	3.27	3.95	3.09	3.15	3.24	3.33	3.05	0.38	0.58	0.78	2.26	1.99	2.28	1.94	1.54
K_2O	-	0.05	0.06	-	0.03	0.06	0.02	-	-	0.03	-	0.09	0.02	0.02	-	0.02
Total	99.96	99.96	99.97	99.98	99.96	99.96	99.96	99.96	99.97	99.97	99.97	99.96	99.95	99.95	99.97	99.97
Si	1.99	1.98	1.98	1.99	1.98	1.99	1.99	1.99	1.97	1.95	1.99	1.99	1.99	1.98	1.99	1.98
Al_{IV}	0.01	0.02	0.02	0.01	0.02	0.01	0.01	0.01	0.03	0.05	0.01	0.01	0.01	0.02	0.01	0.02
Al_{VI}	0.21	0.20	0.16	0.20	0.21	0.20	0.20	0.19	0.03	0.08	0.04	0.16	0.16	0.15	0.13	0.09
Ti	-	-	-	-	0.01	-		0.01	-	-	-	-	-	-	-	-
Fe^{3+}	0.01	0.01	0.04	0.01	-	0.02	0.02	0.02	-	-	0.01	-	-	-	0.01	-
Fe^{2+}	0.16	0.16	0.14	0.17	0.18	0.15	0.17	0.15	0.20	0.17	0.18	0.17	0.19	0.19	0.17	0.18
Mn	-	-	-	-	-	0.01	-	-	-	-	-	-	-	-	-	-
Mg	0.66	0.66	0.68	0.65	0.66	0.66	0.66	0.67	0.77	0.77	0.79	0.70	0.70	0.70	0.72	0.75
Ca	0.76	0.76	0.80	0.75	0.75	0.74	0.74	0.76	0.99	0.93	0.93	0.79	0.81	0.81	0.83	0.86
Na	0.22	0.23	0.21	0.22	0.22	0.23	0.24	0.21	0.03	0.04	0.06	0.16	0.14	0.16	0.14	0.11
K	-	-		-	-	-	-	-	-	-	-	-	-	-	-	-
X_{Fe}	0.20	0.19	0.17	0.21	0.21	0.19	0.20	0.18	0.21	0.18	0.19	0.20	0.21	0.21	0.20	0.19
Jd	21.7	21.9	17.3	21.2	22.0	20.6	21.1	19.6	2.7	4.2	5.3	16.4	14.1	16.1	13.5	10.9
Acm	0.4	1.0	3.4	0.5	-	2.3	2.1	1.7	-	-	0.3	-	-	-	0.2	-
Aug	77.9	77.1	79.3	78.3	78.0	77.1	76.8	78.7	97.3	95.8	94.4	83.6	85.9	83.9	86.3	89.1

Tab. 3. Microprobe analyses of Hb1 (large grains, and inclusions in Grt), and Hb2 (rims around Grt, and from Hb2-Cpx2-Olg symplectites around Cpx1). Grt-Cpx-Czo-Hb±Bt eclogitic amphibolite. Polinik structural complex. PO1 and PO5 samples location according to Fig. 4.

TYPE	Hb^1 in matrix				Inclusions of Hb^1 in Grt				Hb^2 around Grt				Hb^2 from Hb^2±Cpx^2±Olg^2 rims			
Sample	PO5		PO1		PO5		PO1		PO5		PO1		PO5			PO1
SiO_2	49.03	50.81	49.69	49.94	48.57	50.23	48.83	50.44	43.02	39.84	40.90	39.17	50.12	52.79	52.62	49.90
TiO_2	0.63	0.43	0.59	0.52	0.46	0.58	0.67	0.47	0.16	0.06	0.10	0.24	0.23	0.02	0.17	0.45
Al_2O_3	9.18	7.91	8.64	7.83	10.73	8.79	10.07	8.83	16.71	21.02	18.67	19.87	7.42	4.77	5.56	7.49
FeO	10.20	9.44	9.84	10.77	10.60	10.19	1061	9.49	15.50	16.80	17.83	15.40	10.41	9.68	9.37	11.79
MnO	0.20	0.08	0.10	-	-	-	0.04	0.04	0.05	0.17	0.29	0.07	0.14	0.14	0.08	0.25
MgO	15.68	16.39	16.02	16.10	14.56	15.22	15.07	16.27	9.25	6.35	7.20	8.30	15.24	16.60	16.58	14.82
CaO	10.03	10.50	10.74	10.32	10.38	10.40	10.69	10.51	10.66	10.56	10.98	11.14	12.71	13.10	12.52	12.14
Na_2O	2.51	1.70	1.97	1.57	2.07	2.12	1.74	1.77	2.37	2.43	2.16	3.05	1.05	0.42	0.37	0.80
K_2O	0.60	0.46	0.57	0.51	0.52	0.57	0.47	0.53	0.32	0.21	0.11	0.22	0.14	-	0.11	0.13
Total	98.06	97.72	98.16	97.56	97.89	98.10	98.19	98.35	98.04	97.44	98.24	97.46	97.46	97.52	97.38	97.77
Si	6.90	7.12	6.99	7.02	6.86	7.08	6.86	7.02	6.24	5.87	5.99	5.78	7.20	7.51	7.44	7.11
Al_{IV}	1.10	0.88	1.01	0.98	1.14	0.92	1.14	0.98	1.76	2.13	2.01	2.22	0.80	0.49	0.56	0.89
Al_{VI}	0.42	0.43	0.42	0.32	0.64	0.54	0.53	0.47	1.10	1.52	1.21	1.24	0.46	0.31	0.37	0.37
Ti	0.07	0.05	0.06	0.05	0.05	0.06	0.07	0.05	0.02	0.01	0.01	0.03	0.02	-	0.02	0.05
Fe^{3+}	0.73	0.68	0.60	0.94	0.61	0.43	0.70	0.71	0.58	0.54	0.71	0.49	0.08	0.06	0.23	0.47
Fe^{2+}	0.47	0.43	0.55	0.33	0.64	0.77	0.55	0.40	1.29	1.52	1.47	1.41	1.17	1.09	0.87	0.94
Mn	0.02	0.01	0.01	-	-	-	-	-	0.01	0.02	0.04	0.01	0.02	0.02	0.01	0.03
Mg	3.29	3.42	3.35	3.37	3.06	3.20	3.15	3.37	2.00	1.39	1.57	1.83	3.26	3.52	3.49	3.15
Ca	1.51	1.58	1.62	1.55	1.57	1.57	1.61	1.57	1.66	1.67	1.72	1.76	1.95	2.00	1.90	1.85
Na	0.68	0.46	0.54	0.43	0.57	0.58	0.47	0.48	0.67	0.69	0.61	0.87	0.29	0.12	0.10	0.22
K	0.11	0.08	0.10	0.09	0.09	0.10	0.08	0.09	0.06	0.04	0.02	0.04	0.03	-	0.02	0.02
X_{Fe}	0.27	0.25	0.26	0.27	0.29	0.27	0.28	0.25	0.49	0.60	0.59	0.51	0.28	0.25	0.24	0.31
$(Na+K)_A$	0.33	0.13	0.27	0.07	0.23	0.25	0.17	0.14	0.39	0.42	0.39	0.68	0.29	0.13	0.03	0.13
Na_B	0.46	0.42	0.37	0.45	0.43	0.43	0.39	0.43	0.34	0.31	0.24	0.23	0.03	-	0.09	0.12
Name	Hb	Hb	Hb	Hb	Hb	Hb	Hb	Hb	Ts	Ts	Ts	Prg	Hb	Act_{Al}	Hb	Hb

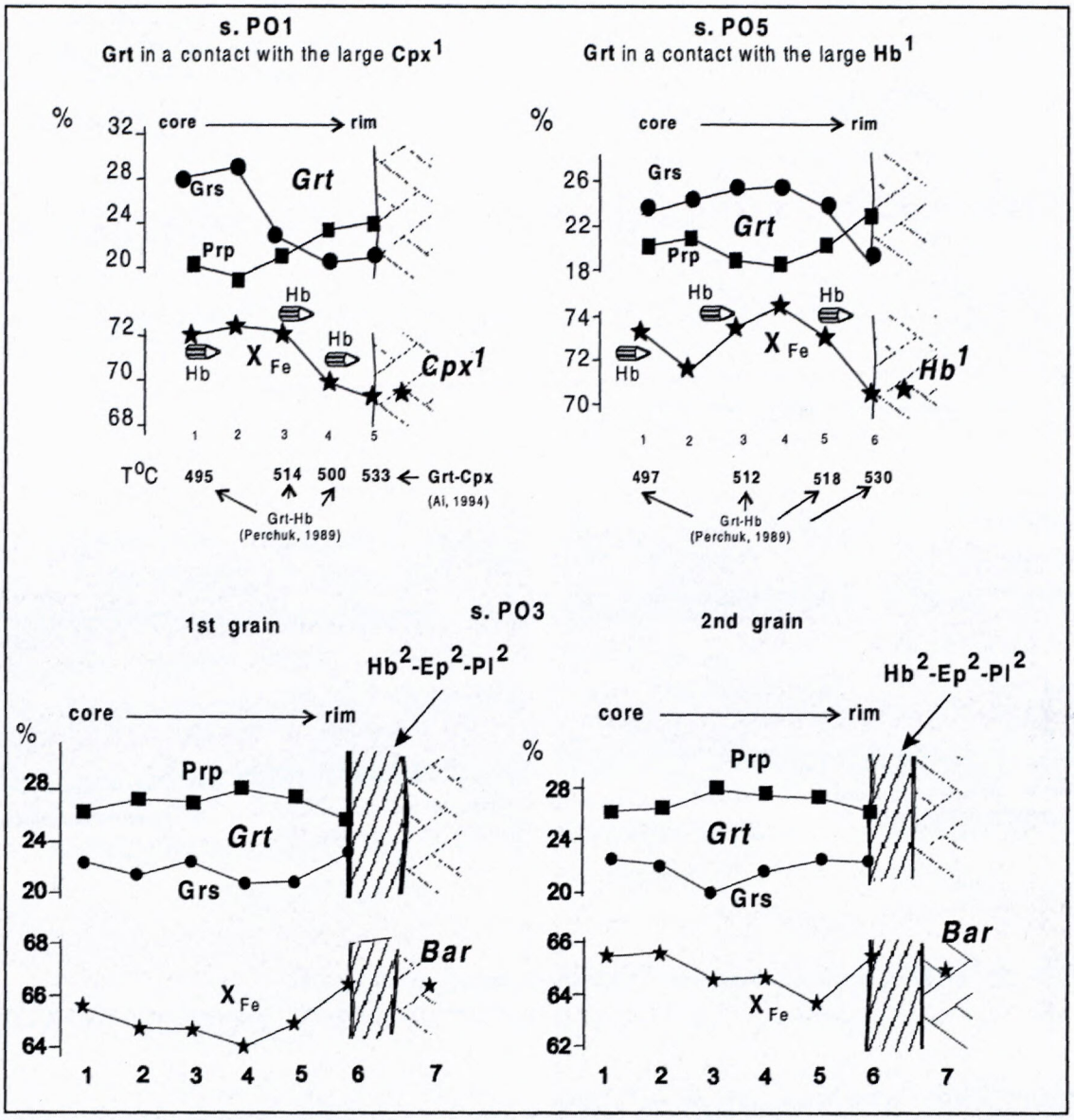

Fig. 6. (a) Compositional profile of Grt grains (s. PO1 and PO5) of HP Na-Aug-bearing eclogitic amphibolite and T estimates of prograde metamorphic stage using Grt-Cpx and Grt-Hb thermometry. The Hb „pencils" indicate places of Hb inclusions along the Grt profile, used for Grt-Hb thermometry. (b) Compositional profile of Grt grains (s. PO3, with indicated Hb inclusions) of Bar amphibolite (a, b - the Polinik structural complex).

(Kleemann and Reinhardt, 1994). We consider the temperatures around 600 °C to be realistic for the pre-Alpine (Variscan) prograde burial stage.

And-Sil gneisses of the Strieden complex (Fig. 5d) also contain snowball-shaped Sil-Bt aggregates, pre-Alpine (Variscan) in age. The recrystallization of this aggregate led to formation of the rounded clusters of fine grains of Cld, Ms and Mgr probably due to reaction of Pl with Sil and Bt. Thus Cld, Ms and Mgr seem to be Alpine (D1, 2) recrystallization minerals of the originally Variscan gneisses. The same newly-formed minerals are observable in the Polinik Ky-Grt gneisses, where they belong to Alpine retrograde or exhumation D2 stage (Hoke, 1990). The temperatures around 500 °C are inferred for the Cretaceous (D1) collision stage of the AA Strieden complex, when the low-medium-T Cld-Mgr-Ms association formed in metapelites of the complex. Such minerals are roughly corresponding to those of the D2 stage found in the Polinik eclogitic and barroisitic amphibolites (Hbl-bearing reactional rims and symplectites) and their host Ky-Grt gneisses, respectively. Because of these similarities and because such aggregates occur as accompanying mylonitic fabrics, the discussed newly-formed mineral assemblage of the Strieden complex is considered to be Alpine (Cretaceous) in age.

5. Microfabrics of quartz and calcite-dolomite mylonites

Thickening of the crust (include the mantle-lithosphere, after Stüwe and Sandiford, 1995) during Cretaceous deformation (e.g. Behrmann and Wallis, 1987; Laubscher, 1989;

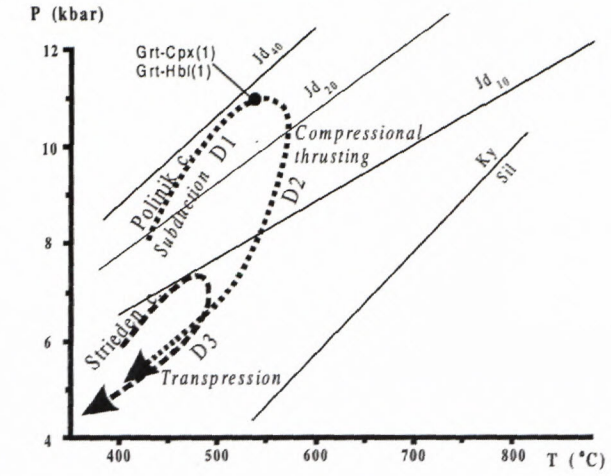

Fig. 7. Estimated P-T-t-paths of the Polinik and Strieden structural complexes in the Kreuzeck Massif (Area 2) based on thermo-barometric estimates (Fig. 6, Tab. 1-3).

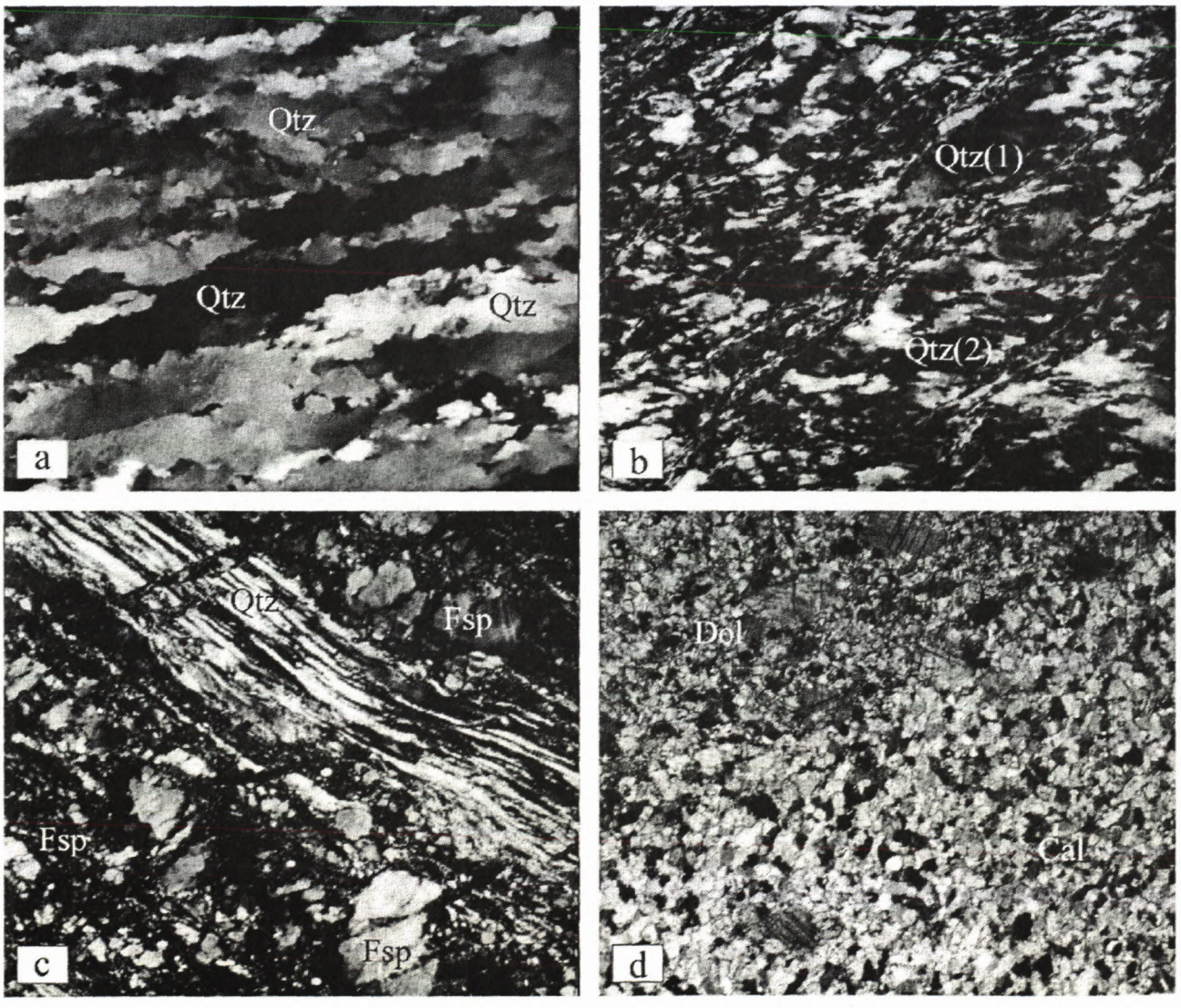

Fig. 8. Microstructures of mylonitic rocks of the Austro-Alpine structural complexes in the Area 2. Sample-location according to Fig. 4. (a) Qtz ribbons of a quartz-layer in gneiss mylonite (sample KR4). (b) Oblique Qtz recrystallized (new) grains indicating top-to-WNW shearing, quartzitic layer in micaschist-gneiss mylonite (s. KR5). (c) Plastic flow in thinned Qtz layer vs. cataclastic flow in Fsp layer, pegmatitic orthogneiss mylonite (s. KR6). (d) Alternation of calcite mylonitic and mylonitic/cataclastic dolomite layers in marble mylonite (s. KR1). (e) Alternation of Qtz and Fsp layers; deformation bands in plastically stretched Fsp layer (dark stripes). (f) Migrative deformation bands boundaries in Qtz. (g) A detail of (e) with two systems of bands: parallel and oblique to mylonitic foliation. (h) EBS image of dolomite porphyroclast with distinct deformation lamellae and core-mantle structure as the evidence of plastic deformation (s. KR1). Magnification: 18x (b, c), 27x (a), 67x (d).

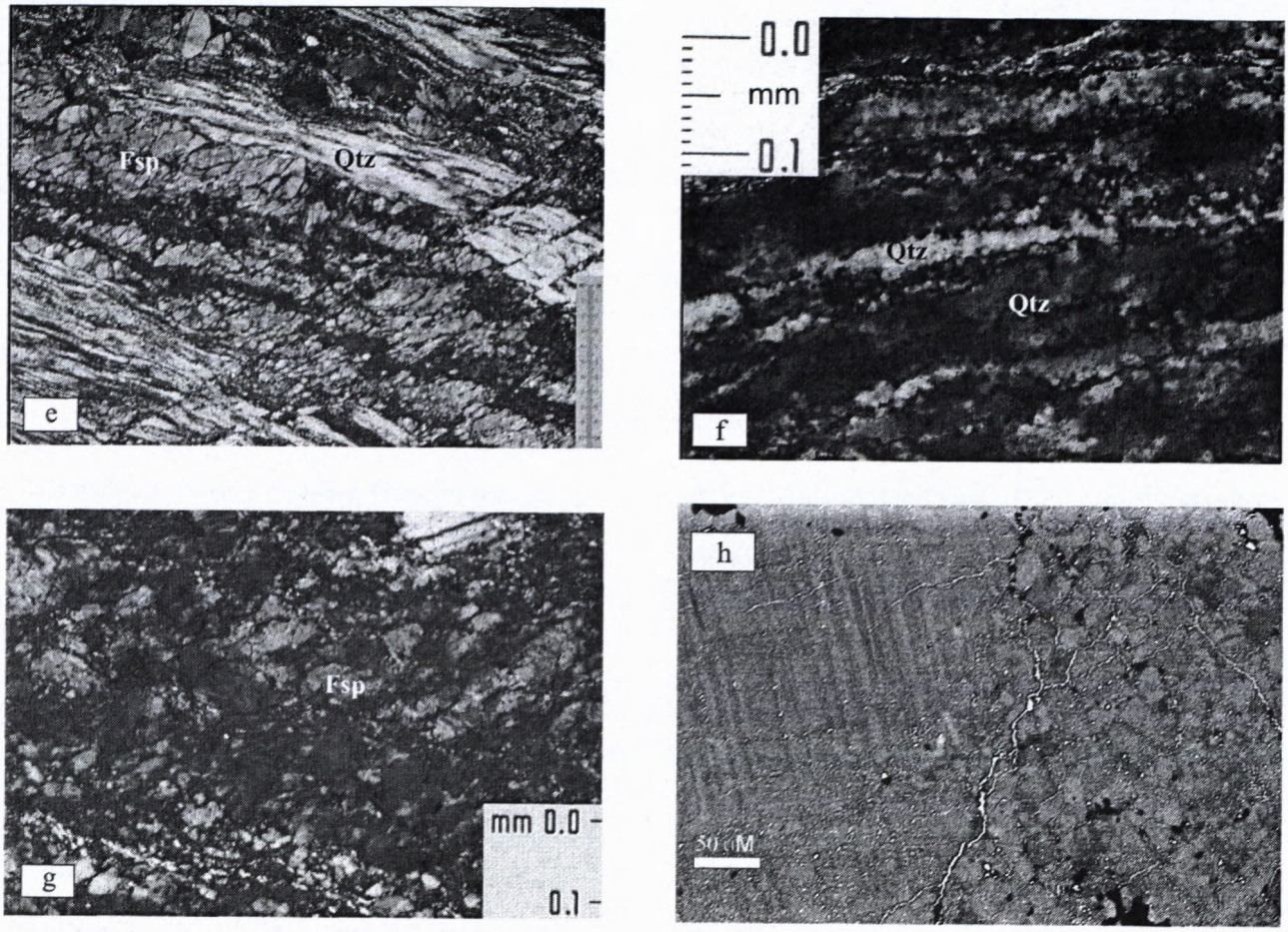

Fig. 8e–h

Tab. 4. Microprobe analyses of zonal Grt surrounded by the Hb2-Ep2-Pl2 rims. Grt-Bar amphibolite. Polinik structural complex. PO3 sample location according to Fig. 4.

	1st Grt grain						2nd Grt grain					
	core					rim	core					rim
SiO_2	38.83	38.55	38.96	38.59	38.80	38.78	38.47	38.46	38.07	38.50	38.08	38.76
TiO_2	0.08	0.13	0.12	0.06	-	0.01	-	-	0.13	0.09	0.08	0.06
Al_2O_3	22.12	22.26	22.11	22.22	21.95	22.07	22.15	22.12	22.02	22.10	21.81	22.02
FeO	23.23	23.41	23.62	23.38	22.91	23.30	23.63	23.64	23.45	23.67	24.25	23.54
MnO	0.61	0.69	0.60	0.50	0.57	0.64	0.60	0.50	0.63	0.49	0.60	0.47
MgO	6.85	6.86	7.29	7.17	7.31	6.81	6.96	7.29	7.14	7.48	7.34	6.61
CaO	8.18	8.03	7.23	7.91	8.34	8.09	8.12	7.87	8.16	7.42	7.70	8.46
Total	99.90	99.93	99.93	99.83	99.88	99.70	99.93	99.88	99.78	99.75	99.86	99.92
Si	3.00	2.97	3.00	2.99	2.99	3.00	2.98	2.98	2.96	2.99	2.96	2.99
Ti	-	0.01	0.01	-	-	-	-	-	0.01	-	-	-
Al	2.00	2.02	2.00	2.02	1.99	2.01	2.01	2.01	2.03	2.02	1.99	2.00
Fe	1.50	1.51	1.52	1.51	1.47	1.51	1,53	1.52	1.52	1.52	1.57	1.52
Mn	0.04	0.04	0.04	0.03	0.04	0.04	0.04	0.03	0.04	0.03	0.04	0.03
Mg	0.79	0.79	0.83	0.82	0.84	0.78	0.80	0.84	0.82	0.86	0.85	0.76
Ca	0.67	0.66	0.60	0.65	0.69	0.67	0.67	0.65	0.68	0.61	0.64	0.70
X_{Fe}	0.66	0.66	0.64	0.65	0.64	0.66	0.66	0.64	0.65	0.64	0.65	0.67
Alm	49.9	50.2	50.8	50.0	48.5	50.2	50.2	50.0	49.6	50.4	50.7	50.5
Sps	1.3	1.5	1.3	1.1	1.3	1.4	1.3	1.1	1.3	1.1	1.3	1.0
Prp	26.3	26.2	28.0	27.3	27.6	26.1	26.4	27.5	26.9	28.3	27.4	25.3
Grs	22.5	22.1	19.9	21.6	22.6	22.3	22.1	21.4	22.2	20.2	20.6	23.2

Slovak Geol. Mag., 8, 1(2002), 65 – 87

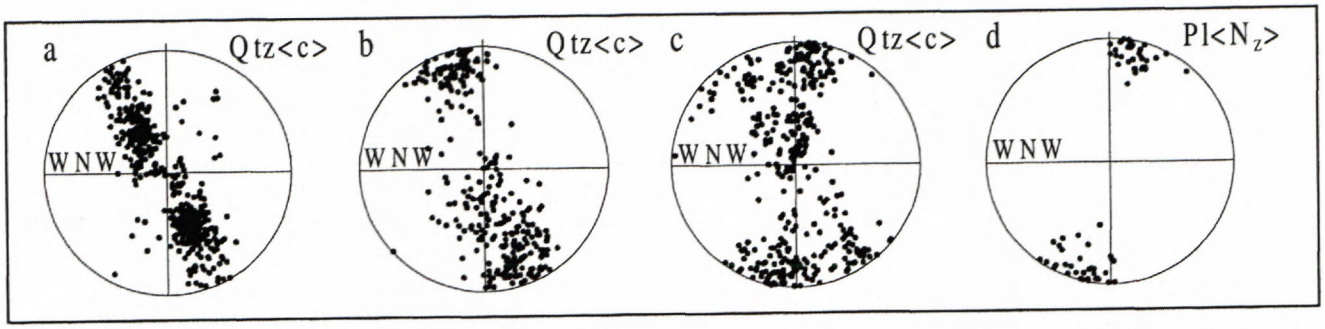

Fig. 9. The U-stage microscope patterns of Qtz and Cal of the Austro-Alpine structural complexes in the Area 2. The microstructures see in Fig. 8a-c. The asymmetric patterns indicate a top-to-W transpressional shear. (a) A rhomb slip in Qtz ribbons, mylonitic gneiss (s. KR4, measured only relic ribbon grains from parallel sections and not recrystallized grains, N=479). (b) Basal <a> slip in Qtz, quartzitic layer in mylonitic gneiss (s. KR5, N=287). (c) Prism <a> and basal <a> slip in Qtz, pegmatitic orthogneiss (s. KR6, N=305). (d) Relic preferred orientation of Pl(Nz) (s. KR6, N=66) indicates (010) [001] slip, pegmatitic orthogneiss.

Ratschbacher et al., 1989; Kurz and Neubauer, 1996; Wallis and Behrmann, 1996; Lammerer and Weger, 1998) resulted in Late Cretaceous to Early Tertiary emplacement of the AA structural complexes (the AA unit) onto the Pennine ones (Fig. 1-4). However, this event can be independent or postdating early-Alpine reactivation of the AA basement structural complexes. Although the radiometric ages are very rare, and most of them point to early Cretaceous exhumation of the AA basement rocks (Thöni and Jagoutz, 1992, 1993; Dallmeyer et al., 1992, 1998), the kinematics of the brittle-ductile exhumation shear zone in the Kreuzeck Massif seems to reflect early-Tertiary reactivation of the AA basement during the final exhumation of HP and MP rocks of the discussed AA Polinik and Strieden structural complexes.

The next part of the paper is devoted to microfabrics of the Polinik (sample KR4) and Strieden (samples KR1 - 6) AA structural complexes in the dextral strike slip shear zone dividing the whole Kreuzeck Massif in the WNW-ESE direction. The western part of this zone was termed by Hoke (1990) as the main mylonite zone (MMZ). This zone seems to be exhumation „suture" of the Polinik and Strieden structural complexes. Moreover, we tried to find principal characteristics of evolution of textural patterns from the Kreuzeck Massif transpression shear zone comparing them to those from the normal-fault shear zone of eastern edge of the Pennine Tauern Window (samples HT 23, 30, 34) (Genser and Neubauer, 1989). The chosen samples represent characteristic diversity of a few tens of studied samples.

5.1. Microfabrics of quartz mylonites from the strike slip shear zone

The *Qtz-rich layers in the light-coloured leucocrate granitic gneiss* (s. KR4) of the Polinik Complex (Fig. 8a) are composed of large flattened Qtz ribbons (Wilson, 1975; Vauchez, 1980; Culshaw and Fyson, 1984; McLelland, 1984) with transitions into dynamically recrystallized grain aggregate.

The U-stage pole-figure (Fig. 9a) shows two maxima at the medium distance from the centre. This pattern is only characteristic for the large Qtz grains visible in form of ribbons and indicates a higher-temperature rhomb slip system dominated during their plastic deformation.

The texture goniometer patterns (Fig. 10/1a,b) however reflect a bulk deformation of the same sample and represent the lower temperature basal <a> slip within the dynamically recrystallized agregate replacing the ribbonous grains.

The straight *Qtz-rich layers in paragneiss* (s. KR5) of the Strieden Complex display a very pronounced preferred orientation of internal obliquely oriented new grains (Fig. 8b). Concentrations of muscovite flakes between the Qtz layers indicate original metamorphic foliation of paragneisses and quartzitic gneisses to muscovite quartzites. The newly-formed internal oblique grains of the Qtz layers exhibit unified extinction with the maximum optical (N_Z//c) direction parallel to prismatic grain boundaries. Asymmetry of newly-formed grains is thus related to non-coaxial strain within the strike slip shear zone (Burg, 1986). The width of grains varies and depends on shape of almost equidimensional, through elongated up to fibrous grains which are sigmoidally rotated into direction parallel with the C-planes (// to former metamorphic foliation). Fine-grained aggregate of Qtz along the C-planes represents narrow zones of high strain localization.

The U-stage pole figure pattern (Fig. 9b) confirms lower temperature non-coaxial deformation and the basal <a> slip system active within recrystallized Qtz layers.

The X-ray texture goniometer patterns (Fig. 10/2a,b) are compatible and also suggest basal <a> slip dominated in a simple shear regime.

Higher deformation rates at lower temperatures are indicated by the contemporary running dislocation creep in Qtz and cataclastic flow in Fsp layers (Fig. 8c) in *mylonitic orthogneisses* (originally pegmatitic veins, s. KR6) of the Strieden complex. The Qtz layers contain extremely stretched fibrous deformation bands. They have clearly migrative boundaries (Fig. 8f) showing dynamic bulging and formation of nearly equidimensional new grains probably due to dynamic rotation recrystallization mechanism (Poirier and Guillopé, 1978; Gleason and Tullis, 1993; Trimby et al., 1998).

Tab. 5. Microprobe analyses of amphiboles: large grains of Bar(=Am1), Ed-Prg and Act =Am2) from Hb2-Act-Olg symplectites; Prg(=Am2) from Hb2-Ep-Olg rims around Grt. Grt-Bar amphibolite. Polinik structural complex. PO3 sample location according to Fig. 4.

Position	LARGE GRAINS IN MATRIX				Hb^2-Act^2-Olg^2 symplectites									HB^2-EP^2-OLG^2 RIMS around Grt		
Name	Bar^1				Ed-Prg^2						ACT^2			Prg^2		
SiO_2	47.43	45.81	47.16	47.87	44.10	43.90	44.49	43.81	41.24	45.10	53.73	52.76	55.21	40.19	40.42	37.78
TiO_2	0.38	0.46	0.46	0.48	0.62	1.06	0.45	0.62	0.19	0.55	0.17	0.15	0.13	0.20	0.17	-
Al_2O_3	13.62	13.35	13.56	14.09	12.40	11.86	13.80	12.66	15.47	11.14	2.59	5.25	1.39	16.87	16.96	20.83
FeO	11.13	12.40	12.16	10.38	14.08	13.46	13.34	13.02	16.39	13.36	11.51	9.32	9.48	15.42	15.72	17.24
MnO	0.21	0.14	0.18	-	0.09	0.01	0.19	0.14	0.13	0.15	0.39	0.13	0.27	0.25	0.17	0.36
MgO	13.19	13.45	13.10	13.22	12.00	12.59	12.07	12.51	10.09	12.85	16.02	16.47	17.90	9.66	9.68	7.54
CaO	8.92	9.19	9.22	8.49	11.73	11.97	10.70	12.04	11.48	12.08	12.73	12.94	12.87	11.66	11.62	10.82
Na_2O	2.94	2.63	2.12	3.25	1.77	1.84	2.28	1.75	2.02	1.76	0.21	0.32	0.17	2.51	2.57	2.93
K_2O	0.46	0.60	0.38	0.52	0.97	0.92	0.87	1.02	1.06	0.66	0.10	0.11	-	1.17	0.87	0.23
Total	98.28	98.03	98.34	98.30	97.76	97.61	98.19	97.57	98.07	97.65	97.45	97.45	97.42	97.93	98.18	97.73
Si	6.64	6.45	6.57	6.68	6.45	6.44	6.40	6.41	6.06	6.58	7.70	7.50	7.82	5.96	5.96	5.57
Al_{IV}	1.36	1.55	1.43	1.32	1.55	1.56	1.60	1.59	1.94	1.42	0.30	0.50	0.18	2.04	2.04	2.43
Al_{VI}	0.89	0.66	0.80	1.00	0.59	0.49	0.74	0.59	0.74	0.50	0.14	0.48	0.05	0.91	0.90	1.19
Ti	0.04	0.05	0.05	0.05	0.07	0.12	0.05	0.07	0.02	0.06	0.02	0.02	0.01	0.02	0.03	-
Fe^{3+}	0.84	1.20	1.14	0.72	0.47	0.39	0.67	0.39	0.77	0.40	0.14	0.05	0.14	0.45	0.54	0.96
Fe^{2+}	0.46	0.25	0.27	0.49	1.25	1.26	0.93	1.20	1.25	1.23	1.24	1.06	0.98	1.46	1.39	1.16
Mn	0.02	0.02	0.02	-	0.01	-	0.02	0.02	0.02	0.02	0.05	0.02	0.03	0.03	0.02	0.04
Mg	2.75	2.82	2.72	2.75	2.61	2.75	2.59	2.73	2.21	2.79	3.42	3.49	3.78	2.13	2.12	1.65
Ca	1.34	1.38	1.38	1.27	1.84	1.88	1.65	1.89	1.81	1.89	1.95	1.97	1.95	1.85	1.83	1.71
Na	0.80	0.72	0.57	0.88	0.50	0.52	0.64	0.50	0.58	0.50	0.06	0.09	0.05	0.72	0.73	0.84
K	0.08	0.11	0.07	0.09	0.18	0.17	0.16	0.19	0.20	0.12	0.02	0.02	-	0.22	0.16	0.04
X_{Fe}	0.33	0.34	0.35	0.31	0.40	0.37	0.39	0.37	0.48	0.37	0.29	0.24	0.23	0.48	0.48	0.57
$(Na+K)_A$	0.24	0.23	0.04	0.24	0.53	0.58	0.47	0.59	0.60	0.53	0.08	0.09	0.03	0.82	0.75	0.75
Na_B	0.64	0.60	0.60	0.73	0.15	0.12	0.33	0.10	0.18	0.09	-	0.02	0.01	0.12	0.14	0.14

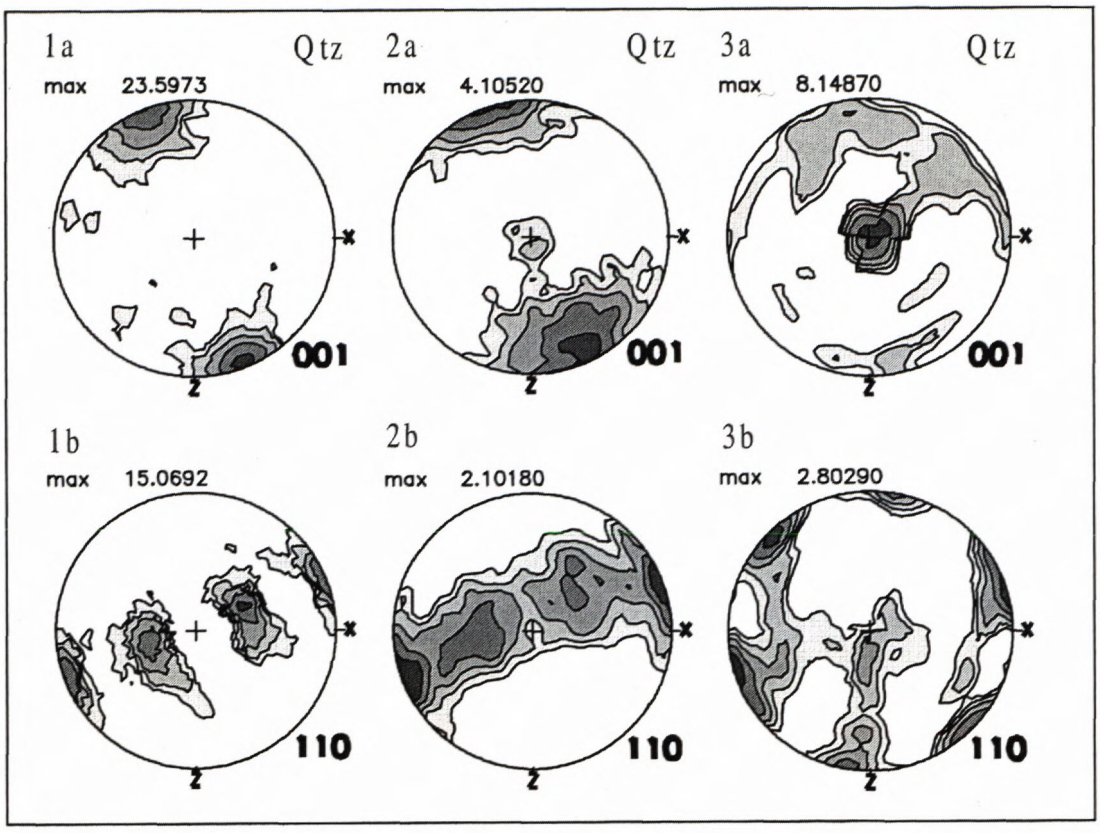

Fig. 10. X-ray texture goniometer patterns of Qtz of the Austro-Alpine structural complex in the Area 2. The microstructures see in Fig. 8a-c. The asymmetric patterns indicate a top-to-W transpressional shear. (1a, b) Basal <a> slip in Qtz of a gneiss mylonite (s. KR4, measured bulk deformation fabric with prevailing recrystallized grains). (2a,b) Basal <a> slip in Qtz, quartzitic layer in mylonitic gneiss (s. KR5). (3a,b) Dominated prism <a> slip in Qtz, pegmatitic orthogneiss (s. KR6).

The cataclastic gouge in Fsp layers seems to be the result of both, the higher strain rates and fluid pressures at the temperatures insufficient for the plastic flow. The Fsp layers and their porphyroclasts however preserve microfabrics of former plastic deformation (Jensen and Starkey, 1985). They are: deformation lamellae, narrow deformation bands with migrative boundaries paralel or oblique to mylonitic/cataclastic foliation (Fig. 8e, g).

The U-stage pole figure of Qtz (Fig. 9c) reflects prism <a> and basal <a> slips in a simple shear regime. The higher temperature stage (at about 500 °C) of plastic deformation of Fsp of some layers is indicated by preferred orientation of Pl N_Z optical directions (Fig. 9d).

The X-ray texture goniometer patterns (Fig. 10/3a,b) confirm a dominated prism <a> slip in Qtz.

5.2. Microfabrics of calcite-dolomite marble mylonites from strike slip shear zone

Boudinaged lensoidal bodies of marbles represent original marble beds within a volcano-sedimentary probably Paleozoic (Strieden) complex. They comprise often undeformed coarse-grained (2-3 mm) Cal-Dol-Tr marbles, which transform to protomylonitic and ultramylonitic marbles towards the inner part of the strike slip shear zone. Dynamic recrystallization reflects active dislocation creep micromechanism of plastic deformation (Fig. 8d). The relict rounded and flattened porphyroclasts exhibit dense deformation lamellae.

The microtexture of mylonitized marbles consists of two different and alternating types of bands or layers (Tab. 6, 7). One type is characteristic by almost homogeneous microtexture built of newly-formed dynamically

Tab. 6. EDS quantification results for dolomite in dolomite marble layer (s. KR1a).

Element	Gross	Net	%Wt	%At Wt	K-Ratio
Ca	928.98	902.39	43.23	26.26	0.71
Mg	357.37	339.92	24.95	24.98	0.21
C	31.10	28.12	0.71	1.44	0.00
O	95.00	91.65	31.11	47.32	0.08
Total			100.00	100.00	

Tab. 7. EDS quantification results for calcite in calcite marble layer (s. KR1b,c).

Element	Gross	Net	%Wt	%At Wt	K-Ratio
Ca	1705.41	1677.56	71.66	50.44	0.95
Mg	29.76	15.50	1.24	1.44	0.01
C	41.85	38.79	0.55	1.29	0.00
O	64.79	61.09	26.55	46.83	0.04
Total			100.00	100.00	

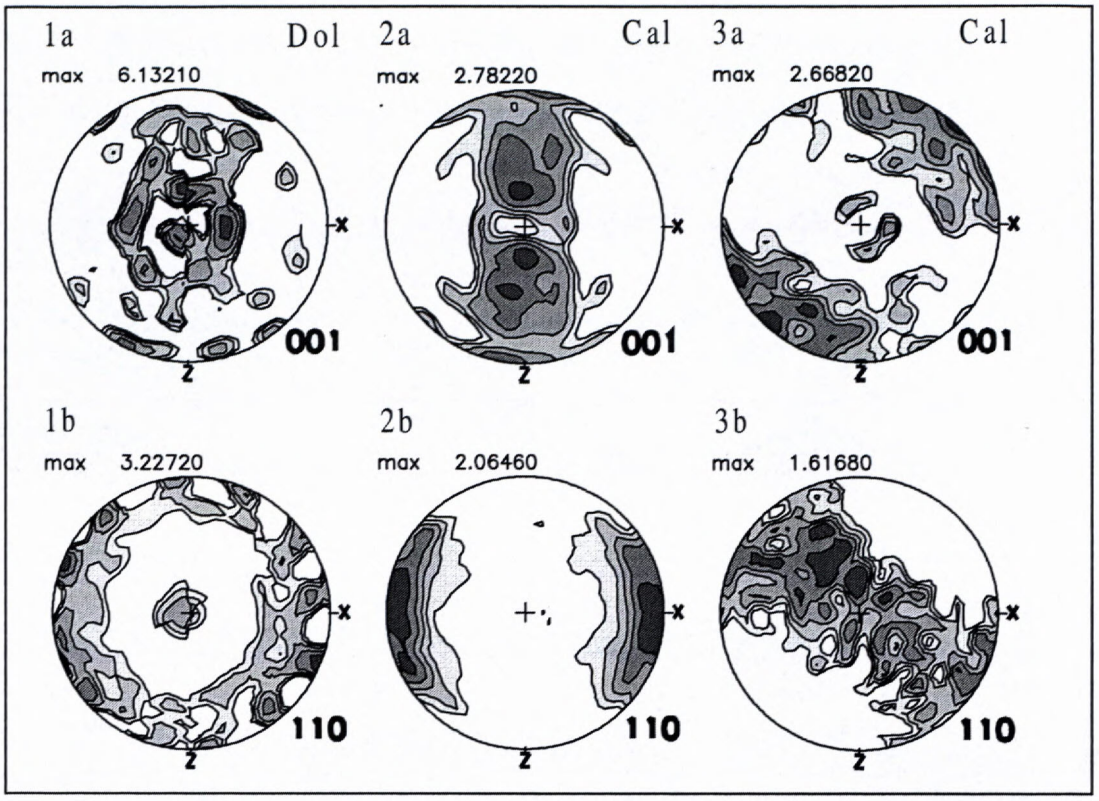

Fig. 11. X-ray texture goniometer patterns of Cal and Dol of the Austro-Alpine structural complex in the Area 2. The layered marble microstructure see in Fig. 8d. (1a,b) Dol pattern combining f-twinning and basal slip at T between 500 and 400 °C in marble layer rich in dolomite (s. KR1a). (2a,b) Almost symmetrical Cal <c> pattern of dynamically recrystallized marble mylonitic layer (s. KR1b). (3a,b) Asymmetrical Cal <c> pattern in dynamically recrystallized marble mylonitic layer (s. KR1c). The asymmetric Cal pattern indicates a top-to-W transpressional shear.

recrystallized equidimensional or polygonal grains with the straight boundaries usually meeting in the triple points. Such a mylonitic microtexture developed in Cal layers and is related to dislocation creep in marble (Nicolas and Poirier, 1976; Lafrance et al. 1994). On the other hand, neighbouring ultramylonitic/ultracataclastic layers are built of fine-grained dolomitic matrix with a lot of Dol porphyroclasts (Fig. 8d). The porphyroclasts show (f-) deformation lamellae and typical core-mantle structures (Fig. 8h) as the result of plastic deformation and dynamic recrystallization of their rims. Most of equidimensional (recrystallized) grains have straight boundaries meeting in the triple points, likewise in the Cal layers. They are often separated by fine-grained ultracataclastic matrix which is missing in the Cal layers. Transition from plastic to cataclastic flow (parallel to C-planes) indicates distinctive micromechanisms of flow applied due to strain partitioning between the Cal and Dol layers at the decreasing temperatures and increasing deformation rates during transpressional uplift.

The X-ray texture goniometer patterns of Dol and Cal (Fig. 11) are different, although representing the neighbouring layers (KR1a - KR1c) of the same sample (KR1). The dolomite layer (KR1a, Fig. 11/1a,b) shows a composite pattern, comprising combined f-twinning and a basal (001) slip. The maxima concentrated around the middle are coeval with the angle relationship of the c-axes and f-twins (Nicolas and Poirier, 1976) subparallel with the horizontal reference line. Whereas the high-angle maxima close to the external part of the circle indicate basal slip active during the dynamic recrystallization of Dol. The neighbouring Cal mylonitic layers document either coaxial pure shear (KR1b, Fig. 11/2a,b), or non-coaxial simple shear (KR1c, Fig. 11/3a,b) in dynamically recrystallized aggregate (Wenk et al., 1987).

A remarkable change of grain size occurred in Cal layers: from 2-3(4) mm to 30-50 μm (Fig. 8d). Some rare Cal porphyroclasts are strongly (e-) twinned. Dol layers consist of distictly (f-) twinned porphyroclasts (200-300 μm in size) surrounded by dynamically recrystallized (20-30 μm) newly-formed grains forming typical „core-mantle" structures (Fig. 8h) within a cataclastic matrix. The width of twin lamellae varies from 5 to 10 μm.

Previously described mylonitic microstructures in Cal (and Dol) aggregates suggest higher differential stresses of plastic deformation (e.g. Schmid et al., 1980; Walker et al., 1990, fig. 18; Rowe and Rutter, 1990; Rutter, 1998, fig. 161.2). Supposing the strain rate between 10^{-12}-10^{-6}.s^{-1} and the temperatures 300-200 °C, and taking into account twinned fabrics overprinted by the dynamically recrystallized aggregates, the estimated differential

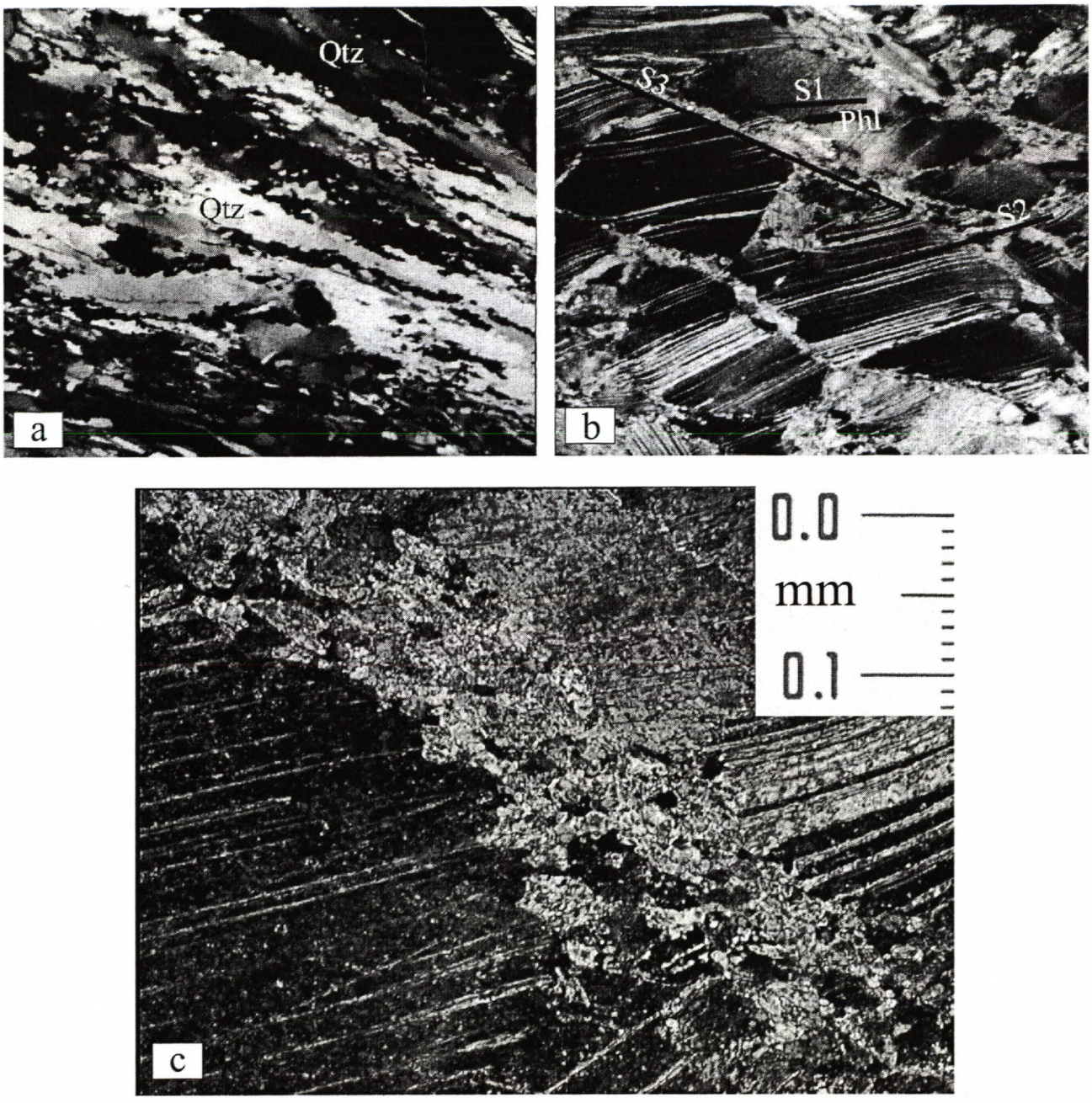

Fig. 12. Microstructures of mylonitic rocks of the Pennine structural complexes in the Area 2. Sample-location according to Fig. 4. (a) Recrystallized Qtz ribbons of „Zentralgneis"-type granitic orthogneiss mylonite (s. HT30). (b) Flattened Cal grains with distinct and parallel e-lamellae fabric cut by shear bands (s. HT23) marked by dynamically recrystallized grains. (c) A detail of ca. 100 μm wide shear band with dynamic aggregate of Cal grains (s. HT23). Magnification: 27x (a), 67x (b).

stresses (> 250 MPa) approach the boundary with high-stress exponential creep.

Thus we found characteristic evolution of microfabrics in high-strain (transpression-type) domains: it starts with deformation lamellae (in both Cal and Dol aggregates), which is easier in coarse-grained marbles. This is in agreement with simple shear experiments in the twinning regime if a single dominant twin orientation is observed, and the non-recrystallized original grains define a grain shape fabric which is oblique to the shear zone boundaries. The twinned grains preserve lobated grain boundaries, which are assumed to represent the higher-temperature grain boundary migration that transforms at higher strains and differential stresses to mechanical twinning (regime 1, Schmid et al., 1980). Later on, minor subgrains and recrystallized grains form along the shear (C) foliation, indicating new strain localization, probably at lower temperatures and higher deformation rates. The latest stage is represented by almost entirely recrystallized twinned porphyroclasts, the relics of which flow within dynamically recrystallized matrix of new Cal grains, indicating an ultramylonitic stage. Mechanical twinning of

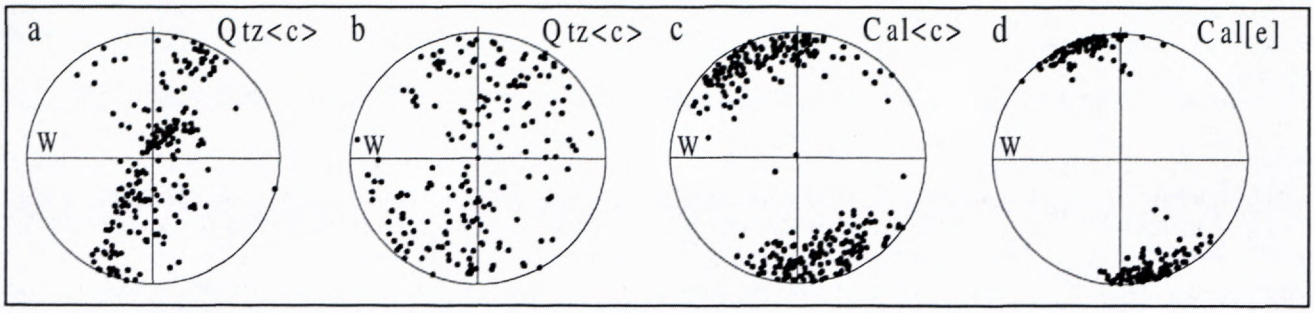

Fig. 13. The U-stage microscope patterns of Qtz and Cal of the Pennine structural complexes in the Area 2. The microstructures see in Fig. 12. The asymmetric patterns indicate a top-to-E extensional sliding. (a) Combined prism <a> and basal <a> slip in Qtz, Zentralgneis-type granitic mylonite (s. HT30, N=223). (b) Basal <a> slip in Qtz, quartzitic layer in marble-mylonite (s. HT23, N=193). (c) Cal <c> fabric of marble-mylonite due to e-twinning dominated (s. HT23, N=300). (d) Cal e-poles pattern, marble-mylonite (s. HT23, N=195).

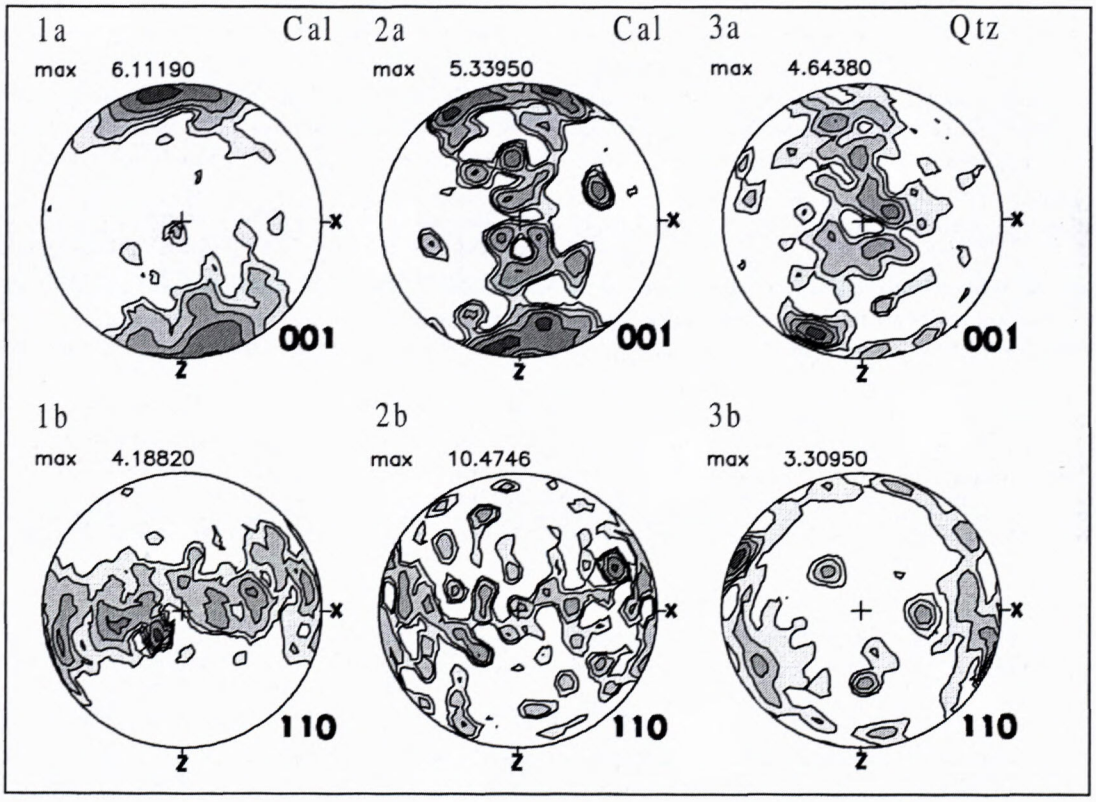

Fig. 14. X-ray texture goniometer patterns of Cal and Qtz of the Pennine structural complexes in the Area 2. The microstructures see in Fig. 12 b,c. The asymmetric patterns indicate a top-to-E extensional sliding. (1a,b-2a,b) Cal fabric of a twinned aggregate in marble-mylonite (1a,b – s. HT23, 2a,b – s. HT34). (3a,b) Combined prism <a>, rhomb and basal slips in Qtz of Zentralgneis-type granitic mylonite (s. HT30).

Cal required higher differential stresses (usually between 180 and 270 MPa, e.g. Rowe and Rutter, 1990) that culminated during superposed dynamic (rotation) recrystallization, thus approaching the boundary of high-stress exponential creep (Walker et al., 1990; Rutter, 1998), providing at last distinct strain softening.

5.3. Microfabrics of quartz and calcite mylonites from normal-fault shear zone

At the eastern edge of the Tauern Window (Fig. 4), a top-to-E extensional transport has been documented by Genser and Neubauer (1989) and dated by Cliff et al. (1985) in the time interval of 25-15 Ma.

The Qtz layers of „Zentralgneis"-type granite-gneisses (Fig. 12a) of the basement, or those of the cover marbles, exhibit distinct mylonitic fabrics. The U-stage (Fig. 13a, b) and X-ray texture goniometer (Fig. 14/3a,b) Qtz c-axes patterns of dynamically recrystallized aggregates are asymmetric. They reflect a basal <a> slip consistent with the top-to-the E extensional normal faulting (sliding).

Microtextures of the deformed marbles usually display 3 planar elements (Fig. 12b): 1. metamorphic (S) foliation defined by white micas and flattened Cal grains,

2. e-lamellae system oblique to S-planes at an acute angle, 3. high-angle shear bands (C-planes) cutting the previous fabrics and parallel to extensional normal fault.

Asymmetric U-stage pole figures of Cal <c> axes (Fig. 13c) and e-normals (Fig. 13d) suggest a top-to the E simple shear (extensional sliding).

Asymmetric to almost symmetric X-ray texture goniometer patterns of Cal (Fig. 14/1a,b-2a,b) reflect deformation twinning in pure to simple shear regime and correspond to bulk flattening of marbles during the subvertical uplift and structural unroofing.

Textural patterns of Cal reflect only the first stage of the uplift deformation i.e. subvertical flattening of original metamorphic grains (400-800 μm of size, with predominating 500-600 μm) and the development of dense and narrow e-lamellae (15-30 μm) oriented at the acute angle to S(shape) foliation. The superimposed shear bands (C-planes) are related to newly-formed zones of strain localization due to an acceleration of deformation or top-to-E extensional sliding of the AA structural complexes from the Pennine ones at the eastern edge of the Tauern Window. Mechanical twinning changed to dynamic recrystallization, producing new grains 15-20 μm in size, excludingly within the about 100 μm narrow shear bands (Fig. 12c). Small grain size suggests high ductile flow stresses. Transition from ductile (dynamic recrystallization) to cataclastic flow, or power-law break up is locally observable in the C-planes of marbles accommodating an extreme exaggeration of deformation at the lowest temperatures of the uplift and exhumation.

6. Discussion on overprint evolution stages

The change of tectonic regime from compressional thrusting to strike slip is evident from the mapped geological structure of the Kreuzeck Massif, registered mesostructures as well as microstructures and related textural patterns of Qtz and Cal. It is inferred to be related to the closing of the Pennine ocean and following continental collision between the Apulia or Adria indenter (with the AA structural complexes) and the European plate. The age of the beginning of lateral strike slip movements (transpression?) is poorly constrained by one 61 Ma datum (K-Ar dating of fine-grained WhM from a mylonite, Waters ex Hoke, 1990). This event might roughly correspond to post-exhumation (from a subduction zone) collisional northward thrusting of the Pennine eclogite-bearing Grossglockner nappe that occurred around 60 Ma (Ar-Ar data on the phengitic WhM, Kurz et al., 1998).

An older, pre-Late-Cretaceous collisional compression and nappe thrusting of the AA structural complexes within the studied area can be inferred mainly from regional subhorizontal boundaries of the 5 crustal sheets or nappes (= structural complexes), thrust one over another, with the clear northern vergency (Putiš, 1998). This event appears to be compatible with practically the whole southern AA domain, and is considered to be Cretaceous (Frank et al., 1987; Thöni and Jagoutz, 1992, 1993; Dallmeyer et al., 1992). The existing mineral K-Ar data from the Kreuzeck Massif indicate an older interval of cooling of the AA basement structural complexes around 90-80 Ma (Hoke, 1990; Oxburg et al., 1966). They are interpreted to reflect a mid-Cretaceous syncollisional exhumation event that changed to lateral strike slip newer basement exhumation period since ca. 70 Ma that is e.g. registered by the mentioned K-Ar data of 66 and 61 Ma in mylonites.

The Adria indenter initiated an extreme reduction of the width of the AA unit mainly due to subvertical transpressional (?) thinning, connected with inferred final exhumation of some early-Alpine HP-MP rocks in the time interval of ca 70 to 40 Ma. This event is constrained by the emplacement of 35-32 Ma old volcanic dykes (Deutsch, 1984) which are not metamorphosed or distinctly deformed. The dykes fill in brittle fractures of mylonitized AA basement structural complexes, being cut by ultracataclasite zones.

Although the ultracataclasites are partly superimposed on mylonites of the MMZ (defined by Hoke, 1990) in narrow newly localized deformation domains, the largest volume of these rocks (include the pseudotachylitic-like types) occurs independently along a megaflexure further to south, dividing the MMZ from subhorizontally stacked and piled basement nappes. This zone branches into shorter partial ultracataclastic domains of variable direction, although two conjugate (fault) systems are prevailing: WNW-ESE and NE-SW in the central part of the Kreuzeck Massif. A similar ultracataclatic zone occurs at the northern margin of the AA structural complexes and is located within the Ragga structural complex south of the Möll river (Putiš et al., 1997b). The zone striking WNW-ESE is subparallel to main Mölltal (in the N) and Oberdrautal (in the S) strike-slip fault zones, which are supposed to have been active since Oligocene, because they are not already cut by the volcanic dykes (ca. 32 Ma).

The HP Polinik and the MP Strieden structural complexes are the AA basement fragments showing the most conspicuous features of Cretaceous-Tertiary reactivation, because both complexes are located along the ductile-brittle strike-slip shear zone (MMZ).

The Polinik and Strieden structural complexes were tectonically emplaced onto the Ragga structural complex showing only greenschist facies LP/LT Alpine reactivation. Thus an inversed Alpine reactivation profile is observable in the Kreuzeck Massif. On the other hand, if one considers the Hochkreuz structural complex as the basis of higher AA nappes (so called the Upper Austro-Alpine, UAA), the discussed shear zone is directly developed at the boundary between the Ragga (LAA?) and Hochkreuz-Steinfeld (UAA) structural complexes. The exhumation „suture„ of the Polinik and Strieden structural complexes having a middle (MAA) position, indicates an extremely shortened domain of the AA basement that was probably subjected to Cretaceous continental subduction. Thus the earlier i.e. early-mid-Cretaceous tectonic evolution of the Kreuzeck Massif might have been connected with the evolution of the Meliata-Hallstatt ocean passive

continental margin. The Late Cretaceous-Tertiary strike slip shear zone and lateral thinning of the AA unit already suggests that the AA crust of the Kreuzeck Massif has become a part of the Pennine ocean active continental margin (Fig. 2).

7. Conclusions

The Austro-Alpine (AA) Polinik and Strieden basement structural complexes of the Kreuzeck Massif (south of the Pennine Tauern Window) bear features of polystage early-Cretaceous and early Tertiary overprint (reactivation) events. They were reconstructed from microstructures of the exhumed HP rocks and the associated mylonitoclasites within a Tertiary strike slip shear zone.

Petrological evolution culminated in HP amphibolite to eclogite facies during the subductional burial (D1, early-Cretaceous?) and changed to MP-LP/MT-LT amphibolite/greenschist-facies during the uplift (D2, mid-Cretaceous). Such a P-T path was estimated in the Polinik structural complex where no relics of pre-Alpine fabrics have been found and both (D1 and D2) stages are Alpine in age. The boundary amphibolite/greenschist-facies MP Alpine overprint was recognized in originally Variscan amphibolite facies assemblages of the Strieden structural complex.

Deformational evolution along the transpression shear zone is characteristic of higher strain rate and a competition between the dislocation creep and cataclastic flow during the (D3) exhumation of studied AA basement fragments. Ductile deformation of feldspar or dolomite aggregates changed to frictional cataclastic flow accompanied by a low temperature quartz and calcite crystal-plasticity. This seems to be a typical frictional-viscous flow (Handy et al., 1999) producing mylonitoclasites (resembling angular pseudotachylites, Curewitz and Karson, 1999) during decreasing temperatures and increasing deformation rates - the process observable in bimineralic or polymineralic high-strained rocks. Associated ultracataclasites fit well to this deformation trend, pointing to a rapid microstructural changes.

Measured textural patterns indicate:

a) Only quartz and calcite deformed ductilely, while feldspar and dolomite were at last subjected to cataclasis within the strike slip shear zone exposed in the Kreuzeck Massif. We found characteristic deformation sequence in calcite aggregate starting with deformation lamellae overprinted by dynamic (rotation) recrystallization. Such a mineral mechanics played an important role during the exhumation of AA basement fragments before an intrusion of volcanic dykes (dated 35-32 Ma) indicating transition to dominated brittle deformation regime, connected later with formation of utracataclasite zones. Therefore frictional-viscous flow seems to be a transitional mechanism from a ductile to frictional (cataclastic) flow within the AA basement rocks located within or closely to strike slip shear zone (MMZ). Asymmetric patterns reflect a top-to-NW thrusting of steeply south-dipping tectonic fragments along the early-Tertiary dextral strike slip shear zone.

b) Miocene extension normal fault of the eastern edge of the Reisseck Massif yielded comparable quartz but different calcite textural patterns (to those from the Kreuzeck Massif) related to a top-to-east structural unroofing of the deeper Pennine unit at the southeastern margin of the Tauern Window. The calcite textural patterns show overprinted deformation lamellae by narrow (ca. 100 μm wide) extension shear bands accommodating newly-localized strain and reflecting a more rapid exhumation. The asymmetry of quartz and calcite textural patterns is in agreement with mesoscopically observable top-to-east sliding along the extensional deformation bands. They are good evidence that ductile deformation persisted until the latest exhumation period of the Pennine unit (before ca. 25-15 Ma, according to Cliff et al., 1985; Selverstone, 1988). In contrast, exclusively (ultra)cataclasites have been developed in the lateral strike slip fault zones of the Kreuzeck Massif AA unit at that time (25-15 Ma). Most of apatite FT ages obtained in both the AA and Pennine units (Staufenberg, 1987; Frisch et al., 1999) already indicate common AA-Pennine very low-temperature history during Oligocene-Miocene strike slip and normal fault tectonics connected with the postcollisional orogen-parallel extrusion of the Apulian (Adriatic) plate fragments (Frisch et al., 2000).

Acknowledgements

This paper was supported: by the Austrian Geological Survey mapping program, VEGA grant of Slovak Republic (No. 1/5228/98 and 1/8248/01, M.P.), Geological Institute of the K.F. University of Graz, Russian Foundation for Basic Research (project # 99-05-64058, S.P.K.). It benefited from research facilities at the Technical University of Denmark (Copenhagen-Lyngby), as well as Villum Kann Rasmussen Fonds for visiting researchers.

References

Ai, Y., 1994: A revision of the garnet-clinopyroxene Fe^{2+} - Mg exchange geothermometer. *Contrib. Mineral. Petrol.* 115, 467-473.

Barber, D.J., 1990. Regimes of plastic deformation - processes and microstructures: an overview. In: Barber, D.J., Meredith, P.G. (Eds.), Deformation Processes in Minerals, Ceramics and Rocks. Unwin Hyman, London, pp. 138-177.

Behrmann, J.H., Wallis, S.R., 1987. Hangendverschuppung des Tauernfenster-Südrandes bei Kals (Osttirol) als Zeuge von eoalpinem Underplating. *Jb. Geol. B.-A.* 130, 133-138.

Berthé, D., Choukroune, P., Jegouzo, P., 1979: Orthogneiss, mylonite and non-coaxial deformation in granites: The example of the South Armorican shear zone. *J. Struct. Geol.* 1, 31-42.

Bezák, V., Kohút, M., Kováčik, M., Madarás, J., Marko, M., Plašienka, D., Putiš, M., 1993. Bericht 1992 Über geologische Aufnahmen im Kristallin der Reisseck-Gruppe auf Blatt 182 Spittal an der Drau. *Jb. Geol. B.-A.* 136, 629-630.

Bezák, V., Kohút, M., Kováčik, M., Madarás, J., Marko, M., Plašienka, D. Putiš, M., 1994. Bericht 1993 Über geologische Aufnahmen im kristallinen Grundgebirge auf Blatt 182 Spittal an der Drau. *Jb. Geol. B.-A.* 137, 523-524.

Bezák, V., Broska, I., Kohút, M., Kováčik, M., Madarás, J., Marko, F., Plašienka D., Putiš, M., Siman, P., 1995. Bericht 1994 Über geologische Aufnahmen im kristallinen Grundgebirge auf Blatt 182 Spittal an der Drau. *Jb. Geol. B.-A.* 138, 551-554.

Blanckenburg, F. von, Davies, J.H., 1996. Feasibility of double slab breakoff (Cretaceous and Tertiary) during the Alpine convergence. *Eclogae Geol. Helv.* 89, 111-127.

Burg, J.P., 1986. Quartz shape fabric variations and c-axis fabrics in a ribbon-mylonite: arguments for an oscillating foliation. *J. Struct. Geol.* 8, 123-131.

Cliff, R.A., Droop, G.T.R., Rex, D.C., 1985. Alpine metamorphism in the south-east Tauern Window, Austria: II. heating, cooling and uplift rates. *J. Metam. Geol.* 3, 403-415.

Culshaw, N.G., Fyson, W.K., 1984. Quartz ribbons in high grade granite gneiss: modifications of dynamically formed quartz c-axis preferred orientation by oriented grain growth. *J. Struct. Geol.* 6, 663-668.

Curewitz, D., Karson, J.A., 1999. Ultracataclasis, sintering, and frictional melting in pseudotachylytes from East Greenland. *J. Struct. Geol.* 21, 1693-1713.

Dallmeyer, R.D., Neubauer, F., Handler, R., Müller, W., Fritz, H., Antonitsch, W., Hermann, S., 1992. 40Ar/39Ar and Rb-Sr mineral age controls for the Pre-Alpine and Alpine tectonic evolution of the Austro-Alpine nappe complex, Eastern Alps. In: Neubauer, F. (Ed.), ALCAPA - Field Guide, Univ. of Graz, pp. 47-59.

Dallmeyer, R.D., Neubauer, F., Handler, R., Fritz, H., Müller, W., Pana, D., Putiš, M., 1996. Tectonothermal evolution of the internal Alps and Carpathians: Evidence from $^{40}Ar/^{39}Ar$ mineral and whole-rock data. *Eclogae Geol. Helv.* 89, 203-227.

Dallmeyer, R.D., Handler, R., Neubauer, F. and Fritz, H., 1998. Sequence of thrusting within a thick-skinned tectonic wedge: evidence from $^{40}Ar/^{39}Ar$ and Rb-Sr ages from the Austroalpine Nappe Complex of the Eastern Alps. *J. Geol.* 106, 71-86.

Dal Piaz, G.V., 1999. The Austroalpine-Piedmont nappe stack and the puzzle of Alpine Tethys. In: Gosso, G., Jadoul, F., Sella, M., Spalla, M.I. (Ed.), *Mem. Sci. Geol.* (Padova), 51/1, 155-176.

Deutsch, A., 1984. Young Alpine dykes south of the Tauern Window (Austria): A K-Ar and Sr isotope study. *Contrib. Mineral. Petrol.* 85, 45-57.

Frank, W., Kralik, M., Scharbert, S., Thöni, M., 1987. Geochronological data from the Eastern Alps. In: Flügel, H.W., Faupl, P. (Eds.), Geodynamics of the Eastern Alps. Deuticke, Vienna, pp. 272-281.

Frisch, W., Brügel, A., Dunkl, I., Kuhlemann, J., Satir, M., 1999. Post-collisional large-scale extension and mountain uplift in the Eastern Alps. In: Gosso, G., Jadoul, F., Sella, M., Spalla, M.I. (Eds.), *Mem. Sci. Geol.* (Padova), 51/1, 3-23.

Frisch, W., Dunkl, I., Kuhlemann, J., 2000. Post-collisional orogen-parallel large-scale extension in the Eastern Alps. Tectonophysics 327, 239-265.

Froitzheim, N., Schmid, S.M., Frey, M., 1996. Mesozoic paleogeography and the timing of eclogite-facies metamorphism in the Alps: A working hypothesis. *Eclogae Geol. Helv.* 89, 81-110.

Genser, J., Neubauer F., 1989. Low angle normal faults at the eastern margin of the Tauern Window (Eastern Alps). *Mitt. Österr. Geol. Ges.* 81, 233-243.

Gleason, G.C., Tullis, J., 1993. The role of dynamic recrystallization in the development of lattice preferred orientations in experimentally deformed quartz aggregates. *J. Struct. Geol.* 15, 1145-1168.

Handy, M., Wissing, S.B., Streit, L.E., 1999: Frictional-viscous flow in mylonite with varied bimineralic composition and its effect on lithospheric strength. *Tectonophysics* 303, 175-191.

Hoinkes, G., Koller, F., Rantitsch, G., Dachs, E., Höck, V., Neubauer, F., Schuster, R., 1999. Alpine metamorphism in the Eastern Alps. *Schweizerische Mineralogische Petrographische Mitteilungen* 79, 155-181.

Hoke, L., 1990. The Altkristallin of the Kreuzeck Mountains, SE Tauern Window, Eastern Alps - Basement crust in a convergent plate boundary zone. Jb. Geol. B.-A. 133, 5-87.

Holland, T.J.B., 1980. The reaction albite=jadeite+quartz determined experimentally in the range 600-1200 grad. C. *Am. Mineralogist* 65, 129-134.

Jensen, L.N., Starkey, J., 1985. Plagioclase microfabrics in a ductile shear zone from the Jotun Nappe, Norway. *J. Struct. Geol.* 7, 527-539.

Kleemann, U., Reinhardt, J., 1994. Garnet-biotite thermometry revised: the effect of Al_{VI} and Ti in biotite. *Eur. J. Mineral.* 6, 925-941.

Kohn, M.Y., Spear, F.S., 1990. Two new geobarometers for garnet amphibolites, with application to southeastern Vermont. *Am. Mineralogist* 75, 89-96.

Kozur, H., 1991. The geological evolution at the western end of the Cimmerian ocean in the Western Carpathians and Eastern Alps. *Zbl. Geol. Pal.*, T. 1, H. 1, 99-121.

Kretz, R., 1983. Symbols for rock-forming minerals. *Am. Mineralogist* 68, 277-279.

Kurz, W., Neubauer, F., 1996. Deformation partitioning during updoming of the Sonnblick area in the Tauern Window (Eastern Alps, Austria). J. Struct. Geol. 18, 1327-1343.

Kurz, W., Neubauer, F., 1998. Eclogite meso- and microfabrics: implications for the burial and exhumation history of eclogites in the Tauern Window (Eastern Alps) from P-T-d paths. *Tectonophysics* 285, 183-209.

Kurz, W., Neubauer, F., Unzog, W., Genser, J., Wang, X., 2000. Microstructural and textural development of calcite marbles during polyphase deformation of Penninic units within the Tauern Window (Eastern Alps). *Tectonophysics* 316, 327-342.

Lafrance, B., White, J.C., Williams, P.F., 1994. Natural calcite c-axis fabrics: an alternate interpretation. *Tectonophysics* 229, 1-18.

Lammerer, B., Weger, M., 1998. Footwal uplift in an orogenic wedge: the Tauern Window in the Eastern Alps of Europe. *Tectonophysics* 285, 213-230.

Laubscher, H., 1989. The tectonics of the Southern Alps and the Austro-Alpine nappes: a comparison. In: Coward, M.P., Dietrich, D., Park, R.G. (Eds.), Alpine Tectonics. *Geological Society London, Special Publications* 45, 229-241.

Leake, B.E., Wooley, A.R., and 20 members of the Subcommittee on Amphibole, 1997. Nomenclature of amphiboles. Report of the Subcommittee on Amphiboles of the Inernational Mineralogical Association Commission on New Minerals and Mineral Names. *Eur. J. Mineral.* 9, 623-651.

Linner, M., 1997. Bericht 1996 über geologische Aufnahmen im Kristallin auf den Blättern 179 Lienz und 180 Winklern. *Jb. Geol. B.-A.* 140, 342-345.

Mancktelow, N.S., Meier, A., Viola, G.A.M., Müller, W., Fügenschuh B., Seward, D., Villa, I.M., 1999. The Periadriatic and adjacent fault systems in the Eastern Alps south and west of the Tauern Window. Abstracts of the 4th Workshop on Alpine Geological Studies, Tübingen. Tübinger Geowissenschaftliche Arbeiten, Series A, 52, 7-9.

McLelland, J.M., 1984. The origin of ribbon lineation within the southern Adirondacks, U.S.A. *J. Struct. Geol.* 6, 147-157.

Neubauer, F., 1994. Kontinentkollision in den Ostalpen. *Geowissenschaften* 12, 136-140.

Nicolas, A., Poirier, J.P., 1976. Crystalline Plasticity and Solid State Flow in Metamorphic Rocks. J.Willey & Sons, London, New York, pp. 216-222.

Oxburg, E.R., Lambert, R.St.J., Baardsgaard, H., Simons, J.G., 1966. Potassium Argon age studies across the southeast margin of the Tauern Window, the Eastern Alps. *Verh. Geol. B.-A.*, 17-33.

Perchuk, L.L., 1989. Intercorrelation of Fe-Mg geothermometers using the Nernst law. *Geokhimia* 5, 611-622 (in Russian).

Plašienka, D., Grecula, P., Putiš, M., Hovorka, D., Kováč, M., 1997. Evolution and structure of the Western Carpathians: an overview. In: Grecula, P., Hovorka, D., Putiš, M. (Eds.), Geological Evolution of the Western Carpathians. *Mineralia Slovaca - Monograph*, Bratislava, pp. 1-24i.

Platt, J.P., 1993. Exhumation of high-pressure rocks: a review of concepts and processes. *Terra Nova* 5, 119-133.

Poirier, J.P., Guillopé, M., 1978. Deformation induced recrystallization of minerals. *Bull. Soc. fr. Minér. Cristallogr.* 102, 67-74.

Powell, R., 1985. Regression diagnostics and robust regression in geothermometer/geobarometer calibration: the garnet-clinopyroxene geothermometer revised. *J. Metam. Geol.* 3, 231-243.

Putiš, M., 1998. Compiled Geological map of the Kreuzeck Massif, Eastern Alps. Austrian Geological Survey, scale 1:25 000, Vienna.

Putiš, M., Bezák, V., Janák, M., Kohút, M., Kováčik, M., Madarás, J., Marko, F., Plašienka, D., 1995. Geological map of the western part of the Kreuzeck Massif, Eastern Alps. Austrian Geological Survey, scale 1:25 000, Vienna.

Putiš, M., Bezák, V., Janák, M., Kohút, M., Kováčik, M., Madarás, J., Marko, F., Plašienka, D. 1996. Geological map of the central part of the Kreuzeck Massif, Eastern Alps. Austrian Geological Survey, scale 1:25 000, Vienna.

Putiš M., Bezák V., Kohút M., Kováčik M., Marko F., Plašienka D., 1997a. Bericht 1996 and 1997 über geologische Aufnahmen im Kristallin auf Blatt 181 Obervellach. *Jb. Geol. B.-A.* 140, 345-348.

Putiš, M., Bezák V., Kohút M., Kovácik M., Marko F., Plašienka D. 1997b. Geological map of the eastern part of the Kreuzeck Massif, Eastern Alps. Austrian Geological Survey, scale 1:25 000, Vienna.

Putiš, M., Fritz, H., Unzog, W., Wallbrecher, E., Korikovsky, S.P., Pushkarev, Y.D., Kotov, A.B., 1998. Exhumation modes of austroalpine eclogite-bearing complexes in the vicinity of penninic windows, Eastern Alps. Abstracts of the XVI. Congress of the Carpathian-Balkan Geological Association, Vienna, Austria, 501.

Putiš, M., Korikovsky, S.P., Pushkarev, Yu.A., 2000. Petrotectonics of an Austroalpine eclogite-bearing complex (Sieggraben, Eastern Alps) and U-Pb dating of exhumation. *Jb. Geol. B.-A.* 142, 73-93.

Putiš, M., Korikovsky, S.P., Wallbrecher E., Unzog, W., Olesen, N.Oe., Fritz, H., 2002. Evolution of an eclogitized continental fragment in the Eastern Alps (Sieggraben, Austria). *J. Struct. Geol.* 24, 339-357.

Ratschbacher, L., Neubauer, F., 1989. West-directed decollement of Austro-Alpine cover nappes in the eastern Alps: geometrical and rheological considerations. In: Coward, M.P., Dietrich, D., Park, R.G. (Eds.), Alpine Tectonics. *Geol. Soc. Spec. Publ.* 45, pp. 243-262.

Ratschbacher, L., Wenk, H.-R., Sintubin, M., 1991. Calcite textures: examples from nappes with strain-path partitioning. *J. Struct. Geol.* 13, 369-384.

Rowe, K.J., Rutter, E.H., 1990. Paleostress estimation using calcite twinning: experimental calibration and aplication to nature. *J. Struct. Geol.* 12, 1-17.

Rutter, E.H.,1998. Experimental dynamic recrystallization of calcite rocks. In: Snoke, A.W., Tullis, J., Todd, V.R. (Eds.), Fault-related Rocks A Photographic Atlas. Princeton University Press, Princeton, New Jersey, pp. 542-543.

Selverstone, J., 1988. Evidence for east-west crustal extension in the Eastern Alps: implications for the unroofing history of the Tauern window. *Tectonics 7*, 87-105.

Schmid, S.M., Paterson, M.S., Boland, J.N., 1980. High temperature flow and dynamic recrystallization in Carrara marble. *Tectonophysics* 65, 245-280.

Spaeth, G., 1997. Bericht 1995 über geologische Aufnahmen im Kristallin der Schobergruppe auf Blatt 179 Lienz. *Jb. Geol. B.-A.* 140, 387-389.

Spear, F.S., 1982. Coexisting calcic amphiboles. Reviews in Mineralogy, v. 9B Amphiboles. In: Veblen D.B., Ribbe P.H. (Eds.), Petrology and Experimental Phase Relations. *Miner. Soc. Am.*, 69-76.

Stampfli G.M. 1996. The Intra-Alpine terrain: A Paleotethyan remnant in the Alpine Variscides. *Eclogae Geol. Helv.* 89, 13-42.

Stampfli G.M., Mosar, J., 1999. The making and becoming of Apulia. In: Gosso, G., Jadoul, F., Sella, M., Spalla, M.I. (Eds.), *Mem. Sci. Geol.* (Padova), 51/1, 141-154.

Staufenberg, H., 1987. Apatite fission-track evidence for post-metamorphic uplift and cooling history of the eastern Tauern window and the surrounding Austroalpine (central Eastern Alps, Austria). *Jb. Geol. B.-A.* 130, 571-586.

Stüwe, K., Sandiford, M., 1995. Mantle-lithospheric deformation and crustal metamorphism with some speculations on the thermal and mechanical significance of the Tauern Event, Eastern Alps. *Tectonophysics* 242, 115-132.

Thöni, M., Jagoutz, E., 1992. Some new aspects of dating eclogites in orogenic belts: Sm-Nd, Rb-Sr, and Pb-Pb isotopic results from the Austroalpine Saualpe and Koralpe type-locality (Carinthia/Styria, southeastern Austria). *Geoch. Cosmoch. Acta* 56, 347-368.

Thöni, M., Jagoutz, E., 1993. Isotopic constraints for eo-Alpine high-P metamorphism in the Austroalpine nappes of the Eastern Alps: bearing on Alpine orogenesis. Schweiz. *Mineral. Petrogr. Mitt.* 73, 177-189.

Tollmann, A., 1977. Geologie von Österreich. Band I: Die Zentralalpen. Deuticke, Vienna.

Trimby, P.W., Prior, D.J., Wheeler, J., 1998. Grain boundary hierarchy development in a quartz mylonite. *J. Struct. Geol.* 20, 917-935.

Vauchez, A., 1980. Ribbon texture and deformation mechanisms of quartz in a mylonitized granite of Great Kabylia (Algeria). *Tectonophysics* 67, 1-12.

Wallis, S.R., Behrmann, J.H., 1996. Crustal stacking and extension recorded by tectonic fabrics of the SE margin of the Tauern Window, Austria. *J. Struct. Geol.* 18, 1455-1470.

Walker, A.N., Rutter, E.H., Brodie, K.H., 1990. Experimental study of grain-size sensitive flow of synthetic, hot-pressed calcite rocks. In: Knipe, R.J., Rutter, E.H. (Eds.), Deformation Mechanisms, Rheology and Tectonics. *Geol. Soc. Spec. Publ.* 54, pp. 259-284.

Wenk, H.R., Takeshita, T., Bechler, E., Erskine, B., Mathies, S., 1987. Pure shear and simple shear calcite textures. Comparison of experimental, theoretical and natural data. *J. Struct. Geol.* 9, 731-745.

Wilson, C.J.L., 1975. Preferred orientation in quartz ribbon mylonites. *Geol. Soc. Am. Bull.* 86, 968-974.

Appendix A

Mineral abbreviations in text and figures (after Kretz, 1983; end-members of Ca-amphiboles after Leake et al., 1997): Ab=albite, Acm=acmite, Act=actinolite, Ads=andesine, Alm=almandine, Am=amphibole, An=anortite, And=andalusite, Ath=anthophyllite, Aug=augite, Bar=barroisite, Bt=biotite, Cal=calcite, Chl=chlorite, Cld=chloritoid, Czo=clinozoisite, Cpx=clinopyroxene, Di=diopside, Dol=dolomite, Ed=edenite, Ep=epidote, Fsp=feldspars, Grs=grossular, Grt=garnet, Hb=horblende (as end member, sensu Leake et al., 1997), Hbl=hornblende, Ilm=ilmenite, Jd=jadeite, Kfs=kalifeldspar, Ky=kyanite, Mgr=margarite, Mnz=monazite, Ms=muscovite, Olg=oligoclase, Omp=omphacite, Phe=phengite, Pl=plagioclase, Prg=pargasite, Prp=pyrope, Px=pyroxene, Qtz=quartz, Rt=rutile, Ser=sericite, Sil=sillimanite, Sps=spessartite, St=staurolite, Tr=tremolite, Ts=tschermakite, Ttn=titanite, Tur=tourmaline, WhM=white mica, WR=whole-rock, Zo=zoisite, Zrn=zircon.